Міністерство освіти і науки України
Національний університет кораблебудування
імені адмірала Макарова
Машинобудівний навчально-науковий інститут

Кафедра двигунів внутрішнього згоряння, установок та технічної експлуатації

«Допущений до захисту»
В.о. завідувача кафедри
Олексій ГОГОРЕНКО
____
« ___» __________ 2023 р.

КВАЛІФІКАЦІЙНА РОБОТА

ВИБІР РАЦІОНАЛЬНОЇ СИСТЕМИ ОХОЛОДЖЕННЯ ДВИГУНА ТИПУ ДМ-185 ДЛЯ КАР'ЄРНОГО САМОСКИДУ

Спеціальність 142 – Енергетичне машинобудування

Для здобуття другого (магістерського) рівня вищої освіти

Керівник роботи Юрій МОШЕНЦЕВ

Здобувач освіти Сергій БЕЗУШКО

Миколаїв 2023

Національний університет кораблебудування
імені адмірала Макарова

Інститут, факультет *Машинобудівний навчально-науковий*
Кафедра *Двигунів внутрішнього згоряння, установок та технічної експлуатації*
Ступінь *Магістр*
Спеціальність *142 Енергетичне машинобудування*
(шифр і назва)
Освітня програма *Двигуни внутрішнього згоряння*

ЗАТВЕРДЖУЮ
Завідувач кафедри *ДВЗ, У та ТЕ*
Олексій ГОГОРЕНКО
«____» ______________ 20___ року

З А В Д А Н Н Я
НА КВАЛІФІКАЦІЙНУ РОБОТУ ЗДОБУВАЧЕВІ ОСВІТИ
Безушко Сергію Олександровичу
(прізвище, ім'я, по батькові)

1. Тема роботи *Вибір раціональної системи охолодження двигуна типу ДМ-185 для кар'єрного самоскиду*

2. Керівник роботи *к.т.н., професор Мошенцев Ю. Л.*,
(прізвище, ім'я, по батькові, науковий ступінь, вчене звання)
затверджені наказом закладу вищої освіти від "___"__________20___ року №________
3. Строк подання здобувачем роботи ________________________
4. Вихідні дані до роботи *Потужність двигуна – 2416 кВт; частота обертання колінчатого валу – 1900 хв$^{-1}$.*

5. Зміст розрахунково-пояснювальної записки (перелік питань, які потрібно розробити) *Застосування системи охолодження двигуна 12ЧН18,5/21,5 на кар'єрному самоскиді БЕЛАЗ-7560; Моделювання робочого циклу двигуна 12ЧН18,5/21,5; Дослідження системи охолодження ЕС12А і створення на результатах дослідження сучасної малопотокової системи 2РК1М.; Розрахунок економічної ефективності від розробки та використання проектованої системи; Охорона праці та навколишнього середовища.*
6. Перелік графічного матеріалу (з точним зазначенням обов'язкових креслень)
Кар'єрний самоскид БЕЛАЗ-7560; Основні параметри для розрахунку системи; Схема типу ЕС12А; Схема типу 2РК1М; Вибір раціональних параметрів системи охолодження типу 2РК1М для двигуна типу 12ЧН18,5/21,5.

7. Консультанти розділів роботи

Розділ	Прізвище, ініціали та посада консультанта	Підпис, дата	
		завдання видав	завдання прийняв

8. Дата видачі завдання____

КАЛЕНДАРНИЙ ПЛАН

№ з/п	Назва етапів роботи	Строк виконання етапів роботи	Примітка

Здобувач освіти _____________ *Сергій БЕЗУШКО*
(підпис) (прізвище та ініціали)

Керівник роботи _____________ *Юрій МОШЕНЦЕВ*
(підпис) (прізвище та ініціали)

Contents

INTRODUCTION

According to the department's assignment, the master's thesis investigates the cooling system of a diesel engine type DM-185 (12FC18,5/21,5 N_e = 2416 kW, n = 1900 rpm), intended for the power unit of the quarry dump truck BELAZ-7560.

The aim of the work is to select the optimal cooling system and determine its rational parameters. To substantiate the choice of the best system, the structural and thermotechnical parameters of the compared systems and all their heat exchangers have been identified.

The Beryslav Machine-Building Plant approached the Internal Combustion Engines Department of the National University of Shipbuilding to conduct a preliminary analysis of the EC12A system. The Internal Combustion Engines Department has extensive experience in developing engine cooling systems, and I was tasked with analyzing the cooling system proposed by the plant based on the department's developments and proposing an alternative system. Thus, the analysis of the proposed cooling system scheme and the development of an alternative variant are relevant tasks.

During the assignment, I utilized pre-existing calculation programs for cooling systems and their heat exchangers, which I had studied in the course "Design of Internal Combustion Engine Cooling Systems" and were provided to me by the department. In addition to the calculation programs for systems and their components, I employed simulation programs for the engine's working cycle in a differential form. These programs were also developed by the faculty members and made available to me for the project. Based on the aforementioned software, I conducted the necessary calculations, generated graphical representations, and justified the selection of the optimal solution.

Based on the conducted work, it was determined that the proposed cooling system, type EC12A, is not the most efficient. An alternative system, type 2PK1M, proposed in the project, allows for a reduction in the mass of all heat exchanger cores in the system by 297 kg (with the total mass of the system's cores being 952 kg). Additionally, the proposed cooling system can achieve the required temperatures of the heat carriers using 32 radiator partitions, while the EC12A -type system requires 46 partitions. The airflow rate in the proposed system is 60 kg/s – 20 kg/s less than in the ES12A system. The proposed system employs a single circuit and a single pump, instead of two circuits and two pumps. The water flow rate is 29.4 kg/s – 6.1 kg/s less. Thus, the proposed system is simpler, less expensive to manufacture, and more cost-effective in operation.

					КРМ.142.6222м.01.01.ПЗ
Зм.	Арк.	№ докум.	Підпис	Дата	

Студент	Безушко С.О.			Section 1 Application of the engine cooling system 12FC18,5/21,5 on the BELAZ-7560 quarry dump truck	Літ.	Аркуш	Аркушів
						7	5
Керівник	Мошенцев Ю.Л.				НУК		
Зав.кафед.	Гогоренко О.А.						

Section 1. Application of the engine cooling system 12FC18,5/21,5 on the BELAZ-7560 quarry dump truck.

The designed cooling system should be installed on a BELAZ-7560 type vehicle. This section discusses the placement of the cooling system in the engine compartment. In addition, various operating modes of the quarry dump truck's engine have been examined, and the design mode, for which the load on the cooling system is the highest, has been identified.

1.1 Brief description of the BELAZ-7560 quarry dump truck.

A quarry dump truck of the BELAZ-7560 type can be equipped with the 12FC18,5/21,5 engine. Currently, it is fitted with an engine with similar specifications. The overall appearance of the career dump truck is shown in Figure 1.1.

Figure 1.1 – Quarry dump truck of the BELAZ-7560.

A career dump truck is designed for transporting bulk materials in a loose state along technological roads in open mining areas with various climate conditions. It can be used in the construction of large industrial and hydraulic structures, the construction of road and highway complexes, as well as in the technological units of processing industry enterprises. Depending on the specific weight of the transported cargo, the highest efficiency is achieved when operated with excavators or loaders with bucket capacities of 45 to 60 m^3 [1]. The main parameters of BELAZ-7560 are presented in Table 1.1.

Table 1.1. Basic parameters quarry dump truck of the BELAZ-7560.

Length, mm	15400
Width, mm	9420
Height, mm	7470
Load capacity	360 tons
Engine	Cummins QSK-78-C
Engine power	2610 kW
Transmission	electromechanical
Torque, N*m/rpm	13771/1500
Specific fuel consumption at nominal power, g/kW*h	201
Tires	59/80R63
Motor-wheel reducer	planetary two-row
Traction electric motor	YJ177B
Traction generator	1TB3030-2GA03
Geometric body volume, m^3	162,8; 139
Turning radius, m	17,2
Dump truck weight without load, kg	261000 (standard configuration)
Full weight of the dump truck, kg	621000
Maximum speed, km/h	64

1.2 Operating conditions quarry dump truck of the BELAZ – 7560.

The operation of a vehicle engine with an electric propulsion system follows a characteristic similar to that of a locomotive (Figure 1.2). On the ordinate axis, you have the engine power, and on the abscissa axis, you have the speed of the dump truck's movement (or wheel rotation frequency). Vertical lines correspond to controller positions or constant crankshaft rotation frequencies of the engine. With an increase in speed at a constant controller position, the engine power can increase up to the maximum value on the external characteristic. In this case, normal engine operation involves increasing power to lower values, as negative aspects in engine parameter changes begin to appear on the external characteristic (such as smoke emission, increased fuel consumption, etc.). In this case, as the load (and speed) increases, the driver waits for some time at the current controller position until the engine parameters allow it. Then, they switch the controller to the next position, and the engine can deliver more power without a significant decrease in key performance indicators. The switching moment can be automated, but, as in conventional vehicles, it relies on the skill of the driver, who "feels" the right moment to change gears.

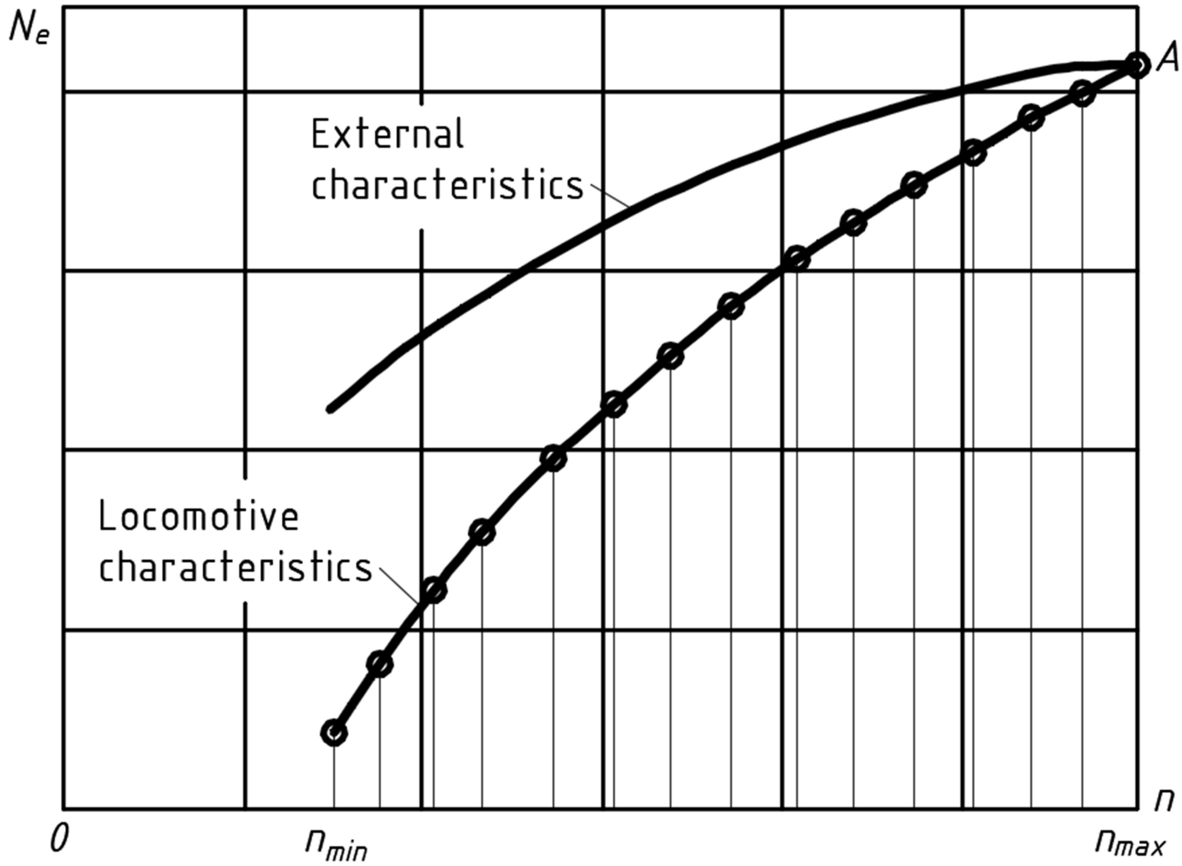

Figure 1.2 – Engine performance characteristics.

Only one characteristic curve is shown, but in reality, there can be many depending on the operating conditions of the vehicle (such as driving uphill, on a rocky terrain, etc.). In all cases, it's important to keep in mind that the engine's RPMs are discrete, and characteristics similar to those found in marine won't apply here. Essentially, the engine operates based on a series of generator characteristics, and changing the frequency is not fundamental. This is done to ensure the coordination of power, RPM, and critical engine parameters (including economic, environmental, etc.). Consequently, providing different power levels is organized at different crankshaft rotation frequencies. Additionally, the movement of a heavy quarry dump truck is associated with sharp fluctuations in external load, which, when directly transmitted, can stop the engine. The electric transmission dampens load fluctuations. Despite all the complexities and peculiarities of the power unit's operation, the engine cooling system experiences the maximum load under nominal operating conditions because the maximum system load is related to the engine's maximum power. It is also evident that the cooling system load is highest under the conditions of the highest ambient temperatures.

Based on this, cooling system calculations should be performed for the engine's nominal power under the highest possible ambient temperatures.

The presented work includes calculations for two cooling system schemes. The first one is proposed by the Berislav Machine-Building Plant (hereinafter referred to as BerMP). The second one is proposed as an alternative to the first. The scheme proposed by BerMP (further denoted as EC12A) does not entirely conform to the canons of an optimally designed cooling system. Its parameters, as expected, could be significantly improved. Full calculations for two cooling systems have been carried out to compare their parameters and select the best scheme. The proposed cooling system, named 2PK1M, with identical thermotechnical parameters, has a heat exchanger core mass of 952 kg, which is 297 kg less than that of the EC12A system. The cooling air flow rate G = 60 kg/s is 20 kg/s less. The water flow rate G = 24.4 kg/s, which is 12.1 kg/s lower.

1.3 The placement of the engine and its cooling system on the BELAZ – 7560 quarry dump truck.

Drawing 1 presents the main views of the BELAZ - 7560. The 12FC18,5/21,5 engine (item 5) is located longitudinally under the hood of the vehicle, meaning the axis of rotation coincides with the direction of movement of the truck. The alternating current generator (item 6) is positioned immediately behind the engine toward the rear axle and is connected to the engine via a driveshaft. The engine cooling system in this drawing is represented by its main components - the radiator (item 3), the fan (item 4), the charge air coolers (item 2), and the oil cooler (item 1). The radiator is traditionally located in front of the engine. A fan is installed between the radiator and the engine, drawing air through the radiator.

Based on the analysis of the dump truck's design, the dimensions of the underhood space where the 2PK1M cooling system is placed have been determined. The dimensions of all heat exchange units of the system were obtained as a result of calculations performed in this study. The nominal engine operating mode was taken as the calculated mode.

As a result of the engine and cooling system components layout in the dump truck's underhood space, it has been established that all components of the power unit are placed adequately. Particularly noteworthy is the proper positioning of the radiator sections of the designed 2PK1M cooling system. The issue is that the space conventionally allocated for radiator placement in automobiles allows for the installation of no more than 32 standard radiator frames. This quantity of frames is precisely obtained in the calculations for the proposed system. For the EC12A system proposed by BerMP, the calculated number of frames is 46, making it impossible to accommodate them in the allocated space on the dump truck.

					КРМ.142.6222м.01.02.ПЗ		
Зм.	Арк.	№ докум.	Підпис	Дата			
Студент		Безушко С.О.			Section 2 Modeling the operating cycle of the 12FC18,5/21,5 engine.	Літ.	Аркуш	Аркушів
							13	13
Керівник		Мошенцев Ю.Л.				НУК		
Зав.кафед.		Гогоренко О.А.						

Section 2. Modeling the operating cycle of the 12FC18,5/21,5 engine.

This section involves modeling the engine's operating cycle. Primarily, it's conducted to determine the components of the heat balance, necessary for the design of the cooling system for the BELAZ-75603 quarry dump truck. Several parameters defining the specifics of the operating cycle were provided by BerMP. However, for a complete modeling of the cycle, these parameters were insufficient and were approximated based on analogs and general considerations of internal combustion engine theory. The list of parameters required for designing the cooling system is presented in Table 2.1.

Table 2.1 Required List of Initial Data for Calculating the ES12A Cooling System.

№	Parameter	Dimension	Description	Note
1.	Ne	kW	Engine power	
2.	n	rpm	Crankshaft rotation frequency	
3.	T_o	K	Ambient temperature	Not provided by BerMP
4.	P_o	kPa	Ambient pressure	Not provided by BerMP
5.	P_1	kPa	Air pressure behind the compressor	
6.	T_1	^oC	Air temperature behind the compressor	
7.	T_s	^oC	Temperature of air in the engine receiver	
8.	$T_{м1}$	^oC	Oil temperature at the oil cooler inlet	Also at the outlet from the engine
9.	$T_{wд2}$	^oC	Water temperature after the engine	
10.	$G_{нв}$	kg/s	Charge air flow	
11.	G_{w1}	kg/s	Water flow in the cold circuit	
12.	G_{w2}	kg/s	Water flow in the hot circuit	
13.	$G_м$	kg/s	Oil flow	Not provided by BerMP
14.	Q_w	kW	Heat flow to water	Not provided by BerMP
15.	$Q_м$	kW	Heat flow to oil	Not provided by BerMP
16.	$G_в$	kg/s	Cooling air flow	Not provided by BerMP
17.	Z_c	pcs	Number of radiator sections	Not provided by BerMP

2.1 Selection of initial parameters for the working cycle calculation of the engine 12FC18,5/21,5.

The simulation of the working cycle of the engine 12FC18,5/21,5 was performed using the Blitz-PRO program developed at the department ICE NUOS. This program allows for the calculation of the main cycle parameters and components of the heat balance with higher accuracy compared to the Grinevetsky-Mazing methodology. Table 2.2 presents the main parameters of engines - analogs to the designed one.

Table 2.2: Main parameters of engines similar to the designed one.

Description	QSK-78-C	20V4000G 63	Cat C 175-16	12FC22/24	12FC26/26
Number of cylinders	18	20	16	12	12
Cylinder diameter, mm	170	170	175	220	260
Piston stroke, mm	190	210	210	240	260
Nominal engine power, kW	2610	2420	3100	2100	2085
Crankshaft rotation frequency, rpm	1900	1500	1800	1200	1000
Specific fuel consumption, g/kW*h	201	198	-	197	220,1
Mean effective pressure, MPa	-	-	-	1,92	-
Engine mass, kg	11640	9290	13041	15400	
Height, mm	2429	2163	2479	2645	3030
Length, mm	3327	3560	4516	4160	5428
Width, mm	1663	1660	1844	1980	1920

Based on the analysis of the parameters of the presented engines and taking into account the recommendations of the internal combustion engine theory, initial data for the calculation of the working cycle were selected and are presented in Table 2.3.

Table 2.3 Initial Parameters for the calculation of the working cycle of engine 12FC18,5/21,5.

№	Param.	Dimension	Value	Description
1	D	m	0,185	Cylinder diameter
2	S	m	0,215	Piston stroke
3	$S_в$	m	0	Stroke of the upper piston of an engine with counter-moving pistons
4	i_z		12	Number of cylinders
5	n	rpm	1900	Engine crankshaft rotation frequency
6	N_e	kW	2416,0000	Effective power at the engine flange
7	a'_{mp}	MPa	0,0450	Coefficients involved in the equation for determining the rela-

№	Param.	Dimension	Value	Description
8	$b'_{тр}$	MPa ·rpm	40,0	tive power of mechanical friction losses
9	λ		0,300	Stroke-to-Bore Ratio
10	k		0,025	Relative De-Axial
11	ε		13	Compression ratio
12	$V_{в.к}/V_s$		2	Ratio of the volume of the portion of the exhaust manifold that combines several cylinders to the working volume of the engine cylinder.
13	i_{z1k}		6	Number of cylinders combined by a common exhaust manifold
14	L_s	m	0,3	Length of intake pipes, the gas flow in which is calculated in a non-stationary setup.
15	d_s	m	0,07	Diameter of intake pipes, the gas flow in which is calculated in a non-stationary setup.
16	$L_к$	m	0,1	Length of exhaust pipes, the gas flow in which is calculated in a non-stationary setup.
17	$d_к$	m	0,07	Diameter of exhaust pipes, the gas flow in which is calculated in a non-stationary setup.
18	$V_{в.р}/V_s$		20	Ratio of the volume of the portion of the air receiver that com-bines several cylinders to the working volume of the engine cylinder.
19	i_{z1p}		12	Number of cylinders connected to a common air receiver of the engine.
20	$\eta_{a.k}$		0,8	Adiabatic efficiency of the compressor.
21	$\eta_{в.t}$		0,8	Internal efficiency of the turbine.
22	$\eta_{m.t}$		0,98	Mechanical efficiency of the turbocharger.
23	μF_t		0,00815	Flow capacity of the turbine (or exhaust pipe in the case of a naturally aspirated engine or a mechanically supercharged en-gine).
24	T_0	K	307	Ambient temperature.
25	p_0	kPa	100	Ambient pressure.
26	$\varphi_{вс}$	%	55	Air humidity before the compressor
27	$\xi_{др}$		1	Pressure ratio behind the throttle to pressure ahead of the throt-tle (for diesel engines - 1)
28	$П_{к1}$		5	Pressure increase factor of the air in the turbocharger №1
29	$П_{к2}$		0	Pressure increase factor of the air in the turbocharger №2
30	Δp_{k1}	kPa	4,022207163	Pressure loss in the intermediate cooler №1
31	$T_{w1онв1}$	K	293	Temperature of the cooling medium at the inlet of the super-charged air cooler №1
32	$\eta_{онв1}$		0,9	Efficiency of the supercharged air cooler №1
33	Δp_t	kPa	8,044414325	Exhaust system resistance (from the turbine outlet of the turbo-

№	Param.	Dimension	Value	Description
				charger №1)
34	$\delta_{вт}$	m	0,015	Conditional average thickness of the cylinder liner wall
35	$\delta_{кр}$	m	0,018	Conditional average thickness of the cylinder head
36	$\delta_{п}$	m	0,022	Conditional average thickness of the piston crown
37	$\lambda_{вт}$	kW/(m·K)	0,035	Thermal conductivity coefficient of the cylinder liner material
38	$\lambda_{кр}$	kW/(m·K)	0,15	Thermal conductivity coefficient of the head material
39	$\lambda_{п}$	kW/(m·K)	0,15	Thermal conductivity coefficient of the piston crown material
40	$R_{ст.вт}$	$(m^2·K)$/kW	0,3	Thermal resistance coefficient of the contamination layer on the liner wall
41	$R_{ст.кр}$	$(m^2·K)$/kW	0,3	Thermal resistance coefficient of the contamination layer on the head wall
42	$R_{ст.пр}$	$(m^2·K)$/kW	0,3	Thermal resistance coefficient of the contamination layer on the piston wall
43	$h_{пр}$	m	0,1	Piston height
44	$h_{о.вт}$	%	100	Length of the cooled part of the liner (in percentage)
45	a_{mpw}		0,5	Fraction of frictional heat dissipated to water/air
46	a_{mpm}		0,5	Fraction of frictional heat dissipated to oil
47	$\alpha_{wвт}$	kW/(m^2·K)	2,5	Heat transfer coefficient from the liner wall to the cooling liquid
48	$\alpha_{wкр}$	kW/(m^2·K)	2	Heat transfer coefficient from the head wall to the cooling liquid
49	$\alpha_{mпр}$	kW/(m^2·K)	0,75	Heat transfer coefficient from the piston walls to the cooling liquid (in case the piston is not cooled by oil, this coefficient takes into account the heat dissipation from the piston crown to the bushing through the rings)
50	$\alpha_{wкар}$	kW/(m^2·K)	0,0001	Heat transfer coefficient from the diaphragm to the crankcase gases
52	$T_{wвт}$	K	343	Average temperature of the cooling liquid in the jacket
53	$T_{wкр}$	K	346	Average temperature of the cooling liquid in the cover
54	$T_{mпор}$	K	363	Average temperature of the oil cooling the piston
55	$T_{wкар}$	K	363	Average temperature of the crankcase gases
56	$a_{вп.к}$		0,01	Coefficients used to calculate the temperature of the intake manifold wall: regular manifold $T_{ст} = T_s + a_{вп.к}T_к + b_{вп.к}$; manifold adjacent to the exhaust system $T_{ст} = T_s + a_{вп.к}T_t + b_{вп.к}$.
57	$b_{вп.к}$	K	5	
58	$d_{э.вп}$	m	0,055	Equivalent diameter of the intake manifold
59	$C_{вп.возд}$		0,6	Correction factor in the formula for the coefficient of heat transfer from the air to the walls of the intake manifold
60	$d_{э.вып}$	m	0,045	Equivalent internal diameter of the exhaust manifold
61	$\delta_{ст.вып}$	m	0,004	Wall thickness of the exhaust manifold

№	Param.	Dimension	Value	Description
62	$\delta_{из.вып}$	m	0,001	Thickness of the insulation layer of the exhaust manifold
63	$\lambda_{ст.вып}$	kW/(m·K)	0,035	Thermal conductivity coefficient of the exhaust manifold wall
64	$\lambda_{из.вып}$	kW/(m·K)	0,005	Thermal conductivity coefficient of the exhaust manifold insulation
65	$R_{ст.вып}$	$(m^2·K)/kW$	4	Thermal resistance of the contamination layer on the inner surface of the exhaust manifold
66	$C_{вып.ог}$		0,35	Correction factor in the formula for determining the heat transfer coefficient from the exhaust gases to the walls of the exhaust manifold
67	$\alpha_{wвып}$	kW/(m^2·K)	0,05	Heat transfer coefficient from the outer wall of the exhaust manifold to the cooling medium (air or water)
68	$T_{wвып}$	K	313	Temperature of the cooling medium (air or water) in the collector
69	$\varphi_{н.впр}$	degree	357	Start angle of injection for the first fuel injection
70	$\varphi_{впр}$	degree	28,00	Duration of injection for the first fuel injection
71	$\delta q_{ц1}$	%	100,00	Fraction of the cycle dose introduced with the first fuel injection
72	$\varphi_{о.вып}$	degree	473	Exhaust Valve Opening
73	$\varphi_{з.вып}$	degree	15	Exhaust Valve Closing
74	$\varphi_{о.вп}$	degree	705	Intake Valve Opening
75	$\varphi_{з.вп}$	degree	215	Intake Valve Closing
76	$\varphi_{п.о.вп}$	degree	80	Intake Valve Duration
77	$\varphi_{п.о.вып}$	degree	80	Exhaust Valve Duration
78	$\varphi_{п.з.вп}$	degree	80	Duration of intake valve closing
79	$\varphi_{п.з.вып}$	degree	80	Duration of exhaust valve closing
80	$D_{вп.кл}$	m	0,065	External diameter of the intake valve
81	$d_{вп.кл}$	m	0,06	Internal diameter of the seat of the intake valve
82	$d_{ст.вп}$	m	0,016	Diameter of the stem of the intake valve
83	$n_{вп.кл}$		2	Number of intake valves
84	$D_{вып.кл}$	m	0,055	External diameter of the exhaust valve
85	$d_{вып.кл}$	m	0,05	Internal diameter of the seat of the exhaust valve
86	$d_{ст.вып}$	m	0,014	Diameter of the stem of the exhaust valve
87	$n_{вып.кл}$		2	Number of exhaust valves
88	$b_{кл.вп}$	m	0,006	Length of the seat forming of the intake valve
89	$b_{кл.вып}$	m	0,006	Length of the seat forming of the exhaust valve
90	$h_{кл.вп}$	m	0,015	Lift height of the intake valve
91	$h_{кл.вып}$	m	0,013	Lift height of the exhaust valve

№	Param.	Dimension	Value	Description
92	$\alpha_{вп.кл}$	degree	45	Angle of the cone of the intake valve disk
93	$\alpha_{вып.кл}$	degree	45	Angle of the cone of the exhaust valve disk
94	$\mu_{вп.к}$		0,784	Flow coefficient of intake organs (minimum value)
95	$\mu_{вып.к}$		0,821	Flow coefficient of exhaust organs (minimum value)
96	g_C		0,873	Mass composition of fuel
97	g_H		0,127	
98	g_S		0	
99	g_O		0	
100	$Q_н$	kJ/kg	42800	Lower heating value of fuel
101	E_a	kJ/kmole	21500	Conditional activation energy
102	B_0		0,000002	Coefficients in Tolstov's formula determining the period of fuel autoignition delay (B_0 = 3,8·10^{-6}; k_n = 1,6·10^{-4}).
103	k_n		0,00016	
104	i_c		9	Number of nozzle orifices
105	d_c	m	0,00035	Diameter of nozzle orifices
106	E_c		1,7	Coefficient in the formula for the mean droplet diameter
107	$A_{z.i}$	s^{-1}	10	Constant for the evaporation time of large droplets
108	ρ_m	kg/ m^3	836	Fuel density at 20 °C
109	μ_m	Pa·s	0,002	Dynamic viscosity of the fuel
110	σ_m	H/m	0,025	Surface tension coefficient of the fuel
111	$\mu_{топл}$	g/mole	230	Molar mass of the fuel
112	$a^{впр}$		6	Coefficients of the functions approximating the fuel delivery process, i.e., determining the form of the functionsσ = σ(φ), dσ/dτ = dσ/dτ(φ). They are the coefficients of two parabolic curves, the sum of which gives the required dependenciesσ = σ(φ), dσ/dτ = dσ/dτ(φ) .
113	$b^{впр}$		1,1	
114	$c^{впр}$		-1,992406081	
115	$m^{впр}{}_1$		1,51	
116	$m^{впр}{}_2$		1,665	
117	$m^{впр}{}_3$		7	
118	$m^{впр}{}_4$		1,75	
119	$\Phi^{впр}{}_1$		0,55	Relative coordinate of the intersection of the first parabolic curve with the abscissa axis
120	$m^{пр}$		0,8	Degree in the correction function equation that takes into account the actual injection conditions, including the influence of the swirling motion of air at the end of compression.
121	$D_ф$		3	Coefficient in the fuel jet range formula
122	L_{cm}	m	0,02	Free-flight length of the fuel jet

№	Param.	Dimension	Value	Description
123	A_{cm}		0,0055	Coefficient in the formula for the angle of the fuel jet cone
124	χ_0		0,5	Minimum degree of reduction in the fuel evaporation rate on the combustion chamber wall
125	a_0	$m^3/(kg{\cdot}s)$	30000	Coefficients of the heat release equation during the fuel supply segment.
126	a_1	s	0,05	
127	a_2	$m^3/(kg{\cdot}s)$	5	
128	m^{n2}		0,5	
129	H		1,25	Vorticity number
130	b_0		0,05	
131	$\Delta\varphi_к$	degree	0,00	Difference between the angle at which the calculation of heat release characteristics concludes using the heat release equations for the fuel injection phase and the angle at which the fuel injection phase ends
132	$\Delta\tau_к$	ms	0,25	Time during which the calculation of heat release characteristics continues, measured from the moment of the end of fuel injection
133	Φ_{z0}		0,6	Relative abscissa coordinate of the minimum of the air charge utilization coefficient function during combustion
134	$\xi_{во}$		0,8	The minimum of the air charge utilization coefficient function during combustion
135	Δ_m		0,01	Relative amount of unburned fuel
136	m		7,8	Index characterizing the combustion process (-0,3...+0,7)
137	X_z		0,999	Fraction of burned fuel
138	B_1		0,002	Proportionality coefficients; δ – fraction of the droplet mass that transforms into a soot nucleus
139	$B_2'\delta$		0,00011	
140	$B_2''\delta$		0,0028	
141	B_3		0,000004	
142	B_4		0,75	Coefficient accounting for the rate of change of local soot concentration with increasing volume
143	n_p		3	Distribution constant characterizing the uniformity of atomization
144	C_1	m/s	2490	The minimum value of the O_2 and N_2 molecule velocity sufficient for the formation of NO_2 through a bimolecular reaction

2.2 The results of the working cycle calculation for the engine 12FC18,5/21,5.

After selecting the initial conditions, multiple variant calculations of the working cycle were performed to achieve the parameters specified by BerMZ in the technical assignment. The calculations were carried out for the engine's nominal operating mode. The results of the final variant are presented in Table 2.4.

Table 2.4 Results of the working cycle calculation for the engine 12FC18,5/21,5.

№	**Param.**	**Dimension**	**Value**	**Description**
1	N_e	kW	2417,00	Effective power at the engine flange
2	M_e	H·m	12148,05	Effective torque at the engine flange
3	$N_{евн}$	kW	2417,00	Effective power of the piston part of the engine
4	$N_{eППК}$	kW	н/д	Power PPK
5	$N_{н.х}$	kW	-134,57	Power of pump strokes
6	N_i	kW	2653,02	Indicated power of the engine (including pump strokes)
7	g_e	kg/(kW·h)	0,2085	Specific effective fuel consumption
8	g_i	kg/(kW·h)	0,1899	Specific indicator fuel consumption (including pump strokes)
9	η_e		0,4034	Effective engine efficiency
10	η_i		0,4653	Indicator engine efficiency
11	η_m		0,8671	Mechanical engine efficiency
12	$П_{к1}$		4,99794	Degree of air pressure increase in turbocharger No. 1
13	$П_{кΣ}$		4,998	Total degree of air pressure increase
14	$\varphi_{сг}$	degree	119,93	Duration of visible combustion of the first fuel portion
15	$\varphi_{з.в}$	degree	1,75	Ignition delay angle of the first fuel portion
16	$\varphi_{з.в2}$	degree	0,00	Ignition delay angle of the second fuel portion
17	$\varphi_{з.в3}$	degree	0,00	Ignition delay angle of the third fuel portion
18	$\varphi_{н.сг}$	degree	358,75	Angle of the beginning of visible combustion of the first fuel portion
19	$\varphi_{dX/d\varphi max}$	degree	382,3	Angle corresponding to the peak on the heat release rate curve
20	$\varphi_{ст}$	degree	358	Moment of flame reaching the first portion of combustion chamber walls
21	$dp/d\varphi_{max}$	kPa/ degr.	492	Maximum rate of pressure rise during combustion
22	$p_{впр}$	bar	2162	Average injection pressure of the first fuel portion
23	d_{32}	mcm	12	Average surface diameter of droplets in the first fuel portion
24	p_z	kPa	18789,45	Maximum combustion pressure
25	T_z	К	1419,72	Maximum combustion temperature
26	p_i	kPa	2416,10	Average indicated pressure (normalized to the entire cycle)

№	Param.	Dimension	Value	Description
27	p_e	kPa	2201,15	Average effective pressure
28	$p_{н.х}$	kPa	-122,55	Average pressure of pump strokes
29	p_s	kPa	484,61	Average air pressure in the receiver (during the intake valve opening)
30	T_s	К	324,39	Average air temperature in the receiver (considering heating during intake)
31	p_c	kPa	18132,28	Mixture pressure at the end of compression
32	T_c	К	937,16	Mixture temperature at the end of compression
33	T_b	К	992,4	Gas temperature at the moment of exhaust valve opening
34	p_b	kPa	1945,2	Gas pressure at the moment of exhaust valve opening
35	T_t	К	754,2	Average gas temperature ahead of the turbine
36	p_t	kPa	510,5	Gas pressure ahead of the turbine
37	$T_{зt}$	К	189,7	Average gas temperature behind the turbine (in the case of sequential supercharging - behind the turbine of turbocharger No. 1)
38	$T_{вс}$	К	316,80	Air temperature behind the intercooler No. 1
39	$p_{вс}$	kPa	496,0	Air pressure behind the intercooler No. 1
40	$T_{рг}$	К	316,8	Temperature of air after mixing with recirculated gases
41	γ_r		0,014	Residual gas coefficient
42	T_r	К	579,8	Residual gas temperature
43	G	kg/s	5,87045	Air/mixture flow through the intake valves of the working cylinder
44	G_t	kg/s	6,00793	Exhaust gas flow (through the engine's exhaust valves)
45	G_{t1}	kg/s	6,00938	Exhaust gas flow through turbocharger No. 1
46	$p_к$	kPa	500,00000	Air pressure behind the compressor
47	$T_к$	К	531,04077	Air temperature behind the turbocharger
48	$\alpha_{гm}$	kW /(m^{2}К)	1,292	Average per cycle heat transfer coefficient from gases to the piston crown and cylinder head
49	$\alpha_{г.вып.m}$	kW/(m^{2}К)	13,457	Average per cycle heat transfer coefficient from exhaust gas to the walls of the exhaust manifold
50	$\alpha_{в.вп.m}$	kW/(m^{2}К)	0,417	Average per cycle heat transfer coefficient from air to the walls of the intake manifold
51	$T_{ст.вт}$	К	493,2	Average temperature of the fire surface of the bushing for the working cylinder
52	$T_{ст.вт.пк}$	К	370,2	Average temperature of the firing surface of the cylinder bushing PPK
53	$T_{ст.кр}$	К	601,9	Average temperature of the fire surface of the lid
54	$T_{ст.пор.ог}$	К	679,6	Average temperature of the fire surface of the piston crown
55	$T_{ст.пор.охл}$	К	600,1	Average temperature of the cooled surface of the piston crown

№	Param.	Dimension	Value	Description
56	$T_{ст.прк}$	К	600,0	Average temperature of the inner surface of the pre-chamber
57	$T_{ст.вып}$	К	752,5	Average temperature of the inner surface of the exhaust manifold
58	$T_{ст.вп.к}$	К	327,1	Inlet manifold wall temperature
59	$\eta_{н}$		1,027	Filling coefficient (related to the full piston stroke)
60	ε'		12,240	Actual compression ratio
61	ΔT_a	К	44,582	Intake air charge heating from the combustion chamber walls
62	$\lambda_{н}$		0,000	filling coefficient PPK
63	φ_a		1,0122	Blowdown coefficient
64	α		2,965138014	Excess air ratio
65	$q_{ц}$	g	0,736716291	Cycle fuel dose
66	$\eta_{а.к1}$		0,8	Adiabatic efficiency of the compressor of turbocharger №1
67	η_{t1}		0,8	Effective efficiency of the turbine of turbocharger №1, determined by the averaged gas parameters in the exhaust manifold and the average flow rate
68	k_{1imp}		1	"Total" impulsivity coefficient of turbocharger №1
69	$N_{к1}$	kW	1337,390597	Power consumed by the compressor of turbocharger №1
70	N_{t1}	kW	1336,96391	Power developed by the turbine of turbocharger №1 taking into account the flow impulsivity
71	$r_{возд}$	%	43,366	Composition of exhaust gases (in volume percentages). For the 8-stroke cycle, the composition is indicated at the moment of opening the exhaust valve of the combustion stroke.
72	r_{N2}	%	50,707	
73	r_{CO2}	%	3,165	
74	r_{CO}	%	0,000	
75	r_{H2}	%	0,000	
76	r_{H20}	%	2,762	
77	δNO_x	%	0,065	Volume fraction of nitrogen oxides in exhaust gases
78		g/ kW·h	6,16	Specific mass fraction of nitrogen oxides in exhaust gases
79		ppm	651,8905322	Volume fraction of nitrogen oxides in exhaust gases (parts per million)
80	[C]	g/m^3	0,007	Volume fraction of soot in exhaust gases
81		%	2,98	Soot content in exhaust gases on the Hartridge scale
82		BOSCH	0,268654823	Soot content in exhaust gases on the BOSCH scale

It should be noted that not all parameters of the presented cycle model correspond to the average values of the respective parameters of modern diesel engines. In particular, the maximum combustion temperature T_z = 1419 K is lower than usual values. This is due to the relatively low power (N_e = 2416 kW) at high supercharging ($\Pi_к$= 5). These parameters could not be changed as they were assigned by BerMP.

The variation of pressure with the crankshaft rotation angle (indicator diagram of the engine) is shown in Fig. 2.1.

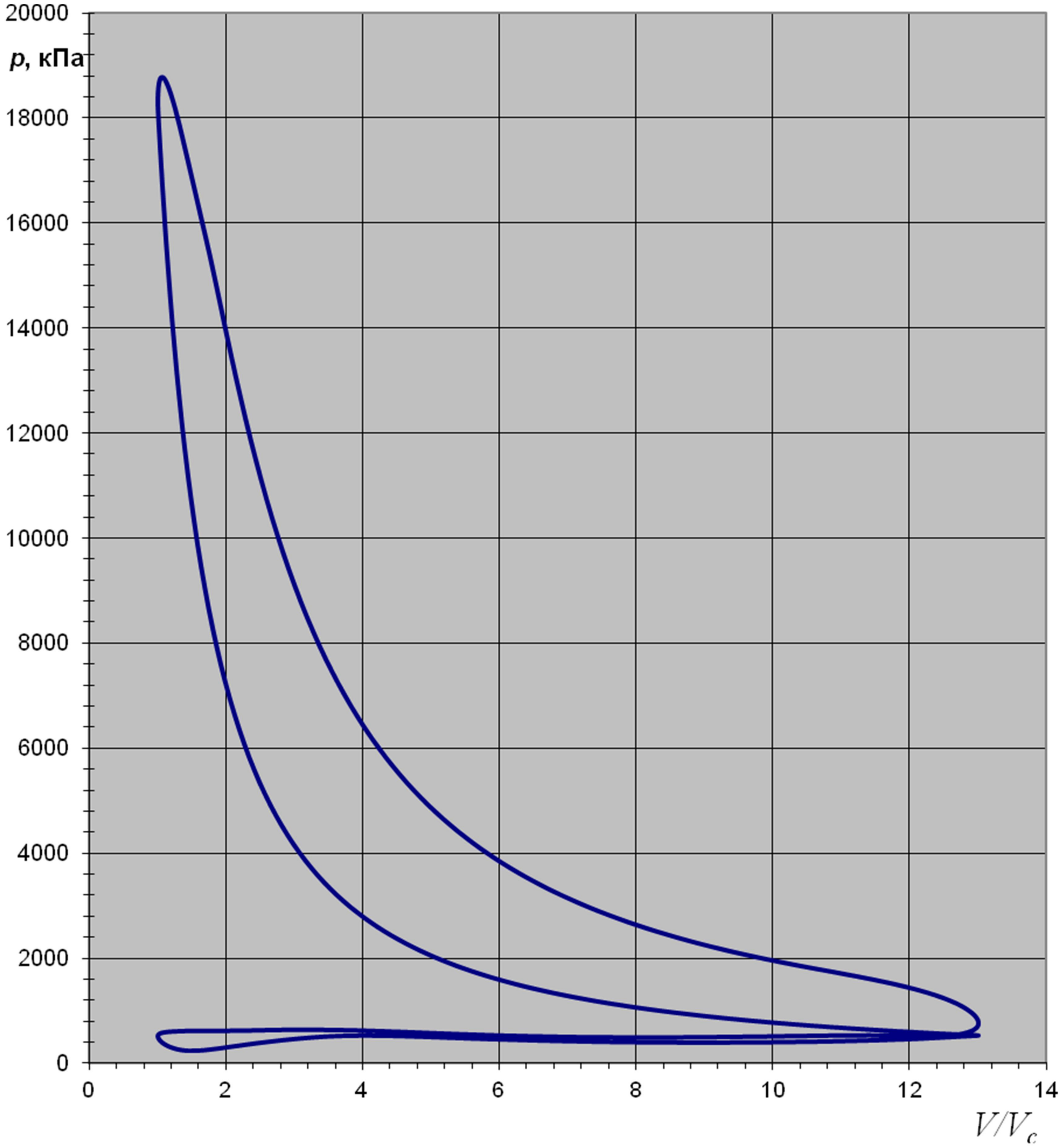

Figure 2.1 - Indicator Diagram of Engine 12FC18,5/21,5.

This combination has led to an unusually high α = 2.96 for the nominal mode. In this case, the temperature could have been increased by increasing the maximum pressure during fuel combustion. However, the calculated P_z = 18.8 MPa is at the upper limit for this class of diesel engines.

The mechanical efficiency of the engine η_m = 0,86, Indicator efficiency η_i = 0,465.

Table 2.5 External Thermal Balance of the Engine.

№	Parameter	Dimension	Value	Description
1	$Q_т$	kW	5990,98	Heat supplied to the cycle during fuel combustion
2	N_e	kW	2417,00	Effective engine power
3	$Q_г$	kW	1613,21	Heat dissipated with exhaust gases
4	$Q_{wто}$	kW	294,15	Heat dissipated to cooling water/air through heat exchange
5	$Q_{wтр}$	kW	118,01	Heat dissipated to cooling water/air due to friction
6	$Q_{w\Sigma}$	kW	402,59	Total amount of heat transferred to cooling water/air
7	$Q_{mтр}$	kW	118,01	Heat dissipated to oil due to moving parts friction
8	$Q_{mпр}$	kW	57,37	Heat transferred from the piston to the oil
9	$Q_{m\Sigma}$	kW	175,38	Total amount of heat dissipated to the oil
10	$Q_{онв1}$	kW	1299,97	Amount of heat dissipated to the charge air cooler 1
11	$Q_{о.вып}$	kW	64,57	Heat dissipated to the walls of the exhaust manifold
12	$Q_{п.вп}$	kW	9,57	Amount of heat transferred to the air from the receiver walls
13	Q_{Σ}	kW	5908,15	Total value

Table 2.6 Initial data for direct calculation of cooling system type EC12A.

№	Parameter	Dimension	Value	Note
1.	Ne	kW	2416	
2.	n	rpm	1900	
3.	T_o	K	37	Not provided by BerMP, accepted at the indicated T_1, T_s
4.	P_o	kPa	100000	Not provided by BerMP, accepted
5.	P_1	kPa	500000	
6.	T_1	°C	250	Probably related to unknown T_o
7.	T_s	°C	45	Probably related to unknown T_o
8.	$T_{м1}$	°C	96	
9.	$T_{wд2}$	°C	108	

№	Parameter	Dimension	Value	Note
10.	$G_{нв}$	kg/s	5,87	It is accepted as revised due to an apparent error by BerMP
11.	G_{w1}	kg/s	11,1	
12.	G_{w2}	kg/s	24,4	
13.	$G_{м}$	kg/s	14	Not provided by BerMP, accepted after analysis and simulation
14.	Q_{w}	kW	403	Not provided by BerMP, accepted after analysis and simulation
15.	$Q_{м}$	kW	175	Not provided by BerMP, accepted after analysis and simulation
16.	$G_{в}$	kg/s	80	Not provided by BerMP, accepted according to prototype
17.	Z_{c}	pcs	46	Not provided by BerMP, accepted according to prototype

As a result of the working cycle calculation of the engine 12FC18,5/21,5, parameters essential for subsequent cooling system calculations have been obtained. They are presented in Table 2.6. The calculation results show no significant deviations from commonly accepted standards in modern engine engineering.

Зм.	Арк.	№ докум.	Підпис	Дата

КРМ.142.6222м.01.03.ПЗ

Студент	Безушко С.О.			
Керівник	Мошенцев Ю.Л.			
Зав.кафед.	Гогоренко О.А.			

Section 3
Analysis of the capabilities of a full-flow cooling system for the EC12A and design low-flow System 2PK1M

Літ.	Аркуш	Аркушів
	27	37

НУК

Section 3. Analysis of the capabilities of a full-flow cooling system for the EC12A and design low-flow System 2РК1М.

The Bereslavsky Machine-Building Plant (BerMP) provided a series of technical parameters for the designed full-flow cooling system. The technical requirements provided by BerMP contain several significant inaccuracies in key parameters. For example, the air supercharging flow rate (a value that can be relatively easily and accurately determined given the known engine type, its power, boost pressure, and rotation frequency) is given with a considerable deviation from the potentially correct value.

3.1 Initial data for calculation EC12A type system.

The cooling system schematic (fig. 3.1) for convenience has been designated as EC12A.

<u>Parameters provided by BerMP:</u>

Engine type: diesel 12FC18,5/21,5

1. $Ne = 2416$ kW
2. $n = 1900$ rpm
3. $P_к = 500$ kPa, single-stage supercharging
4. $G_{нв} = 3,6$ kg/s
5. $T_к = 250\ ^oC$
6. $T_s = 45\ ^oC$
7. $T_{м1} = 96\ ^oC$
8. $T_{м2} = 90\ ^oC$
9. $T_{wм1} = 70\ ^oC$
10. $T_{wм\ 2} = 80\ ^oC$
11. $T_{w3} = 83\ ^oC$ (hot circuit)
12. $T_{w1} = 35^oC$ (cold circuit)
13. $G_{w2} = G_{wд} = 88$ м^3/ h (hot circuit) = 88000/3600 = 24,44 kg/s
14. $G_{w1} = 40$ м^3/ h (cold circuit) = 40000/3600 = 11,11 kg/s

15. Dimensions of the charge air cooler unit no more than $L \times B \times H$ = 633×380×359mm.

From the analysis of the provided materials (a part of which is presented below), it can be concluded that they are incomplete and not sufficiently systematized. The complete set of parameters required for the calculation of practically any engine cooling system is fundamentally known. Such a set is established based on the experience of designing engine cooling systems by various organizations, including the Internal Combustion Engines Department of the National University of shipbuilding. It depends on the calculation scheme and the type of task (direct or reverse calculation). Table 3.1 provides a complete set of initial data required for the direct calculation of the EC12A type system.

As evident from the table and notes, several important parameters are missing. Considering that obtaining all the necessary data with the required precision is currently impossible, these missing data have been assumed based on the available initial data and comprehensive mathematical modeling.

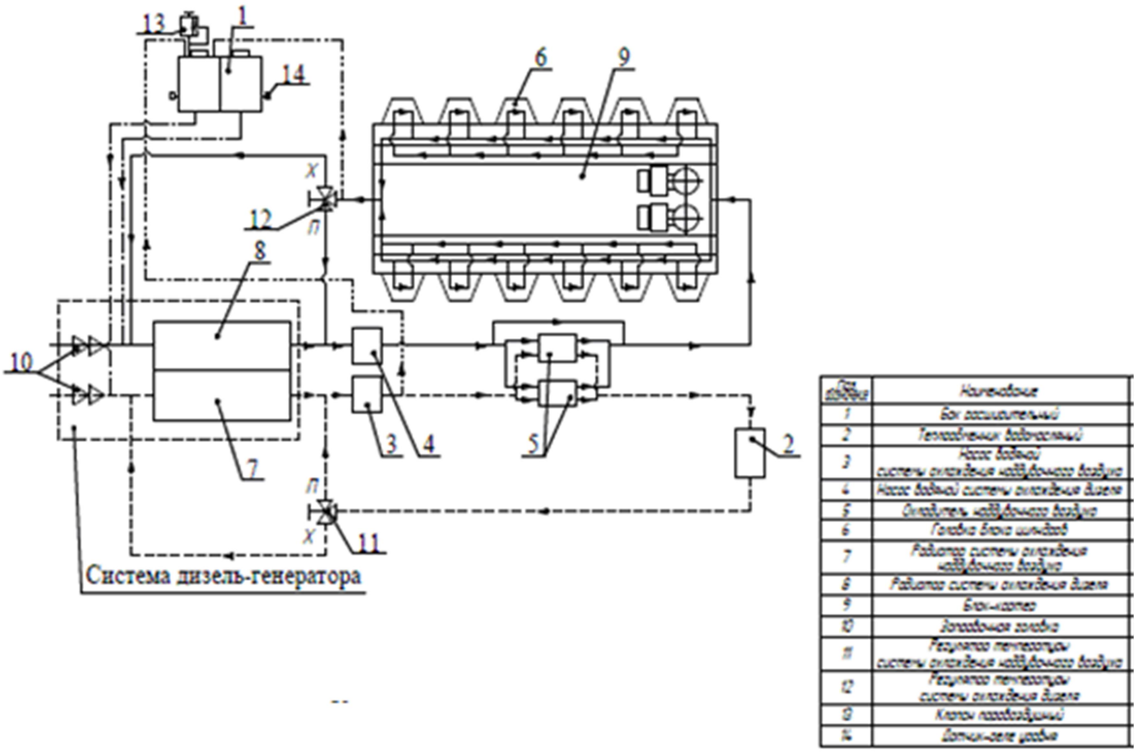

Figure 3.1. Diagram of the EC12A type, a variant proposed by the factory, engine type 12FC18,5/21,5, N_e = 2416 kW, n = 1900 rpm.

Table 3.1. Essential List of Initial Data for Calculating the Cooling System of the EC12A Type.

№	Parameter	Dimension	Description	Note
1	N_e	kW	Engine power	
2.	n	rpm	Crankshaft rotation frequency	
3.	$T_о$	К	Ambient temperature	Not provided by BerMP
4.	$P_о$	kPa	Ambient pressure	Not provided by BerMP
5.	P_1	kPa	Air pressure behind the compressor	
6.	T_1	^oC	Air temperature behind the compressor	
7.	T_s	^oC	Temperature of air in the engine receiver	
8.	$T_{м1}$	^oC	Oil temperature at the oil cooler inlet	Also at the outlet from the engine
9.	$T_{wд2}$	^oC	Water temperature after the engine	
10.	$G_{нв}$	kg/s	Charge air flow	
11.	G_{w1}	kg/s	Water flow in the cold circuit	
12.	G_{w2}	kg/s	Water flow in the hot circuit	
13.	$G_м$	kg/s	Oil flow	Not provided by BerMP
14.	Q_w	kW	Heat flow to water	Not provided by BerMP
15.	$Q_м$	kW	Heat flow to oil	Not provided by BerMP
16.	$G_в$	kg/s	Cooling air flow	Not provided by BerMP
17.	Z_c	pcs	Number of radiator sections	Not provided by BerMP

* Notes to the table.

In addition to the parameters specified in the table, it is necessary to provide:

1. The maximum allowable resistances of all heat exchangers for both coolants (not provided by BerMP).

2. The cooling system diagram with a description (provided by BerMP, Fig. 3.1).

3. Information on the method of heat dissipation from the cooling system: the nature of the radiators, their arrangement relative to the fan, the airflow rate of the fan (cooling air), the maximum resistance of the radiators, and the fan shaft. A diagram and description of the fan system are desirable (not provided by BerMP)

The cooling system diagram for use in computational schemes should be transformed. Naturally, it should not differ fundamentally from the scheme proposed by

BerMP. Such a variant is presented in Fig. 3.2. The system diagram corresponds to the BerMP drawing, but it includes labels convenient for subsequent calculation. Additionally, the diagram includes a radiator device in the form of blocks R1 and R2 equipped with fan. Also, a bypass is installed in the scheme, allowing water to bypass the oil cooler with a bypass flow rate $G_{п1}$. This bypass is installed to optimize the scheme, which was developed in one of the calculations.

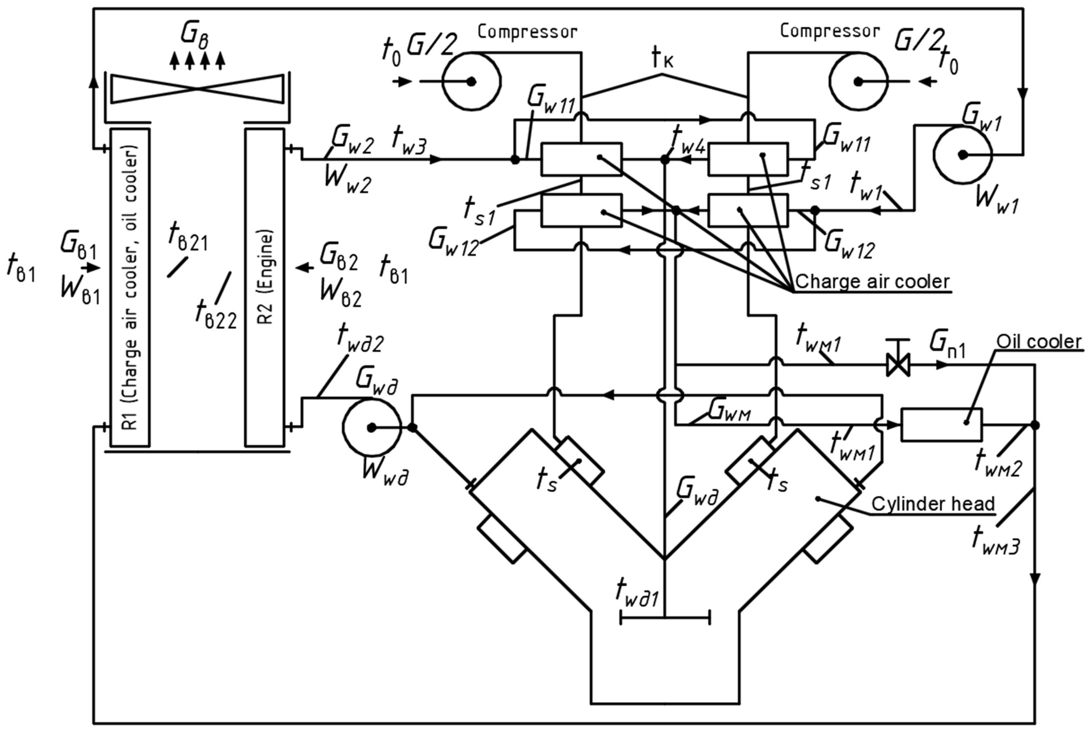

Figure 3.2. Diagram of the cooling system of EC12A, revised in the project and adapted for calculation purposes.

3.2 Analysis of parameters presented by BerMP.

What is accepted, rejected or clarified.

The numbering of parameters corresponds to the numbering of the parameters provided by BerMP above.

Parameters 1, 2, and 3 are accepted.

Parameter 4 is clearly erroneous. Given the specified parameters 1...3, its value can be relatively easily determined, and according to our calculations, it should be equal to 5.87 kg/s (clarifications may be needed due to a lack of information about the engine, but the air flow rate will still be close to the stated value).

Thus, we reject the specified air flow rate and accept the refined value $G_{нв}$ = 5,87 kg/s.

Parameters 5, 6, 7, 8 are accepted.

Parameters 9 and 10 are not crucial, and there is no need to satisfy them. At the same time, they provide interesting information and are used below for a computational analysis.

Parameters 11 and 12 are not crucial, although T_{w1} = 35°C provides information about the potential efficiency of the cold circuit radiator and the possible ambient temperature (not specified in BerMP). These parameters are not critical for BerMP and may not be satisfied.

Parameters 13 to 15 are accepted.

Thus, parameters 1, 2, 3, 5, 6, 7, 8, 13, 15 are unequivocally accepted. Parameter 4 is rejected and replaced with the refined value.

Parameters 9 and 10 are accepted partially, taking into account the temperature difference between them.

Parameters 11 and 12 will be used for analysis; their compliance is not crucial.

As a result of the analysis of the provided BerMP parameters and the mathematical modeling of the engine, the set of initial data has values given in Table 3.2.

Table 3.2. Initial data for the direct calculation of the cooling system of the EC12A type

№	**Parameter**	**Dimension**	**Value**	**Note**
1	Ne	kW	1416	
2	n	rpm	1900	
3	T_o	K	37	Not provided by BerMP, accepted
4	P_o	kPa	100000	Not provided by BerMP, accepted
5	P_1	kPa	500000	
6	T_1	^oC	250	
7	T_s	^oC	45	
8	$T_{м1}$	^oC	96	
9	$T_{wд2}$	^oC	108	
10	$G_{нв}$	kg/s	5,87	Accepted as clarified, due to an obvious mistake by BerMP
11	G_{w1}	kg/s	11,1	

12	G_{w2}	kg/s	24,4	
13	$G_{м}$	kg/s	14	Not provided by BerMP, accepted after analysis and simulation
14	Q_w	kW	403	Not provided by BerMP, accepted after analysis and simulation
15	$Q_{м}$	kW	175	Not provided by BerMP, accepted after analysis and simulation
16	$G_{в}$	kg/s	80	Not provided by BerMP, accepted according to prototype *
17	Z_c	pcs	46	Not provided by BerMP, accepted according to prototype

*The maximum possible flow rate $G_{в}$ with the given number of radiator posts is determined by the maximum permissible air resistance of the posts, which is 60 mm water column.

Analysis of some initial data.

1. There is an opinion that cooling system calculations should be carried out for the most severe operating conditions. From the standpoint of minimal possible heat dissipation in the system, these conditions correspond to the highest ambient temperatures. The BerMP does not specify the conditions for such temperatures, but it provides a range of temperatures directly related to T_o. Therefore, it is necessary (while adhering to the specified T_1 and T_s) to calculate T_o, which is the reference temperature for the manufacturer's manual.

Since the BerMP specifies the values of T_s and T_1, they can be correlated with the ambient temperature, as this correlation is unique and exists. Considering these temperatures, it can be established (based on modeling, taking into account the probable efficiencies of the charge air cooler, compressor, and turbine) that the ambient air temperature will be equal to $T_o = 34\ ^oC$.

2. Since the cooling air flow rate Gв is not specified in the BerMP, we set it to a value commonly used for serial mainline locomotives with similar engine power: $G_в = 80$ kg/s.

3. The type and parameters of the radiator device in the BerMP are not specified. We assume that the radiator is organized based on a standard radiator device for locomotives (assembled from standard uprights). The number of uprights is limited to the value commonly used for serial mainline locomotives: $Z_c = 46$ pcs.

4. Analysis of oil consumption data $G_{м}$ and heat flow into the oil $Q_{м}$.

Based on the provided parameters, it can be established that the heat flow into the oil (and it can be calculated using the formula below) amounts to

$$Q_м = G_{w2} C_{pw} (T_{wм2} - T_{wм1}) = 465090 W.$$

Oil consumption should be (with a possible error in the oil specific heat value)

$$G_м = \frac{Q_м}{C_{pм} (T_{м1} - T_{м2})} = 37,27 \text{ kg/s}$$

Energy consumption of the oil flow

$$W_м = G_м C_{pм} = 77515 \text{ W /К}$$

Energy consumption of the water flow

$$W_{wм} = G_{w2} C_{pw} = 46509 \text{ W /К}$$

The efficiency of the oil cooler should be equal to

$$\eta_{мо} = \frac{T_{м1} - T_{м2}}{T_{м1} - T_{wм1}} \frac{W_м}{W_{м\min}} = 0,3846$$

At the same time, oil consumption (volumetric) for engines of the DM 185 type with a different power is provided.

$Q'_{м1500}$ = 630 l/min,

$Q'_{м3745}$ = 1176 l/min,

Accordingly

$G_{м1500}$ = 9,072 kg/s

$G_{м3475}$ = 16,93 kg/s

Proportionally to these numbers (by power), you can roughly estimate the oil consumption for our engine. It can be equal to

$G_{м2416}$ =10,9...14,6 kg/s

In this case, the oil consumption we calculated earlier is significantly overestimated (37.27 kg/s). At the same time, the heat flow into the oil will also be overestimated. It should be noted that the calculated values by us unequivocally correspond to the data presented by the БерМР, but they contradict other figures provided by them in various technical specifications for these engines.

The heat flow into the oil, assuming the estimated oil consumption values, will be

$$Q_{м2416} = 136{,}3...182{,}3 \text{ kW}.$$

To resolve the situation, the engine cycle was simulated using the differential form developed at NUOS. The simulation yields figures very close to those obtained by proportion. The most probable figure is

$$Q_{м2416} = 175{,}4 \text{ kW},$$

which falls within the established values and corresponds to the most probable engine cycle at the given power, RPM, and boost pressure.

Therefore, the oil consumption and heat flow into the oil should be accepted based on the modeling data, as the data provided by the BerMP are evidently erroneous.

Accepted

$$Q_{м2416} = 175{,}4 \text{ kW},$$

Accordingly, the oil consumption calculated by the formula and corresponding to the modeling data is accepted

$$G_{м} = \frac{Q_{м}}{C_{pм}(T_{м1} - T_{м2})} = 14{,}05 \text{kg/s}$$

5. System diagram. Transformed for convenience in calculations. Deviations from the BerMP scheme are associated with the addition of conditional names of parameters, the connection of the radiator device, and the introduction of a bypass with a flow rate of $G_{п1}$. The bypass allows for different flows through the charge air cooler and oil cooler. In this case, it is assumed to vary the flow of the cold circuit pump G_{w1}.

6. Constraints on the dimensions of the charge air cooler (not exceeding L×B×H = 633×380×359 mm) are understood as follows:

L – depth (dimensional length of the charge air cooler along the airflow). When calculating the bundle, it is necessary to take into account the difference in dimensions between the bundle and the dimensional dimensions. Typically, the bundle size is smaller by approximately 10%, i.e., L ≈ 570 mm.

B – dimensional width of the charge air cooler (dimension perpendicular to the airflow and the axis of the water channels of the bundle). B ≈ 360 mm.

H – height of the charge air cooler(dimension along the axis of the water channels). For the bundle, it is the distance between the tube sheets. H ≈ 310 mm.

Thus, the calculated dimensions of the combined bundle (charge air cooler of the hot and cold circuits) should not exceed L×B×H = 570×360×310 mm.

3.3 Cooling System Calculation EC12-A.

For the calculations of the system, a computational complex was developed, consisting of the following blocks:

thermal scheme calculation block of the system;

calculation block of hot circuit charge air cooler;

calculation block of cold circuit charge air cooler;

calculation block of radiator R1;

calculation block of radiator R2;

calculation block of oil cooler .

The performed calculations do not include blocks that are included in more detailed calculations:

engine calculation block and its thermal balance;

hydraulic calculations block of the system;

aerodynamic calculations block of the system.

The last blocks, during the system calculations, provide variable parameters. In simplified calculations, these parameters are taken as averages and constants.

The thermal system calculation block is formed in accordance with the methodology developed at the department. It is based on a system of 19 basic equations and 15 additional expressions that reflect the features of the proposed scheme. The specified system of equations is solved using the reverse problem scheme (with some deviations from the classical scheme; in particular, the oil cooler in this problem is considered by direct calculation, i.e., its data are adjusted to other system parameters). In the reverse problem, the design parameters of all heat exchangers are set, initial data on flows and initial parameters of coolants in the system are specified, and heat flows into water and oil are defined. Temperatures at control points are determined.

All calculation blocks are interconnected during calculations with direct and inverse connections.

The task of calculating the cooling system of the type EC12A can be mainly classified as an inverse problem since the design parameters of the charge air cooler and both radiators are set. At the same time, the design parameters of the oil cooler are not set but calculated based on the determined parameters of coolants before and after the oil cooler during the problem solution. Such a situation already classifies the problem as mixed, and the reason for such a formulation is related to a practical approach to solving this problem, where the design of the oil cooler is the least constrained by the imposed restrictions.

In the presented table, the efficiency of the system for cooling the supercharged air is calculated using the formula

$$\eta_{co} = \frac{T_к - T_s}{T_к - T_{w1}}.$$

The data from Table 3.2 is taken as the initial input. Additional constraints, following the current standards, are considered:

Air resistance of one unit of the charge air cooler system, made in one housing, not exceeding 500 mm water column.

Air resistance of radiator sections, not exceeding 60 mm water column.

Resistance of all water heat exchangers - not more than 60 kPa.

Resistance of the oil cooler for oil - not more than 250 kPa.

Water velocities in the heat exchangers - not more than 1.5 m/s.

The maximum dimensions of the two combined bundles should not exceed L×B×H = 570×360×310 mm.

Formulation of the calculation task for the EC12A system: calculate the EC12A system with the maximum possible compliance with the initial data provided by BerMZ.

Questions regarding the task:

1. Can the specified temperatures T_s, $T_{wд2}$, $T_{м1}$ be achieved with the given initial parameters and imposed constraints?

2. Is it possible to improve the obtained parameters, and how can this be achieved?

3. How can the efficiency of the cooling system be characterized?

4. What parameters should the cooling system and its heat exchangers have to achieve all specified temperatures of the heat carriers (T_s, $T_{wд2}$, $T_{м1}$)?

General Considerations in Performing Variant Calculations.

All heat exchangers are based on types of heat exchange surfaces that can be manufactured and applied in practice. Therefore, further considerations on the appropriate ratio of dimensions for hot and cold circuit charge air cooler are based on the parameters of the selected heat exchange surface. The same applies to the dimensions and masses of radiators and oil coolers.

The choice of $\eta_{нв11}$ determines the water temperatures before and after the engine, $T_{wд1,2}$. The higher the $\eta_{нв11}$, the higher the water temperatures $T_{wд1,2}$ before and after the engine. Increasing $\eta_{нв11}$ leads to a decrease in $\eta_{нв12}$, since the overall air resistance is limited. The overall length is also limited, although the limit for air resistance occurs at much shorter bundle lengths than the limit for this size. As a result, the lower the $\eta_{нв11}$, the higher the $\eta_{нв12}$ will be. Apparently, the result of these relationships is that a decrease in $\eta_{нв11}$ leads to a decrease in t_s. This is confirmed by the calculations performed.

Results of the calculation.

Table 3.3 Results of the calculation for the EC12-A system.

Parameter	Dimension	Variants		Description
		1	2	
$Q_д$	kW	402,6	402,6	Heat flux to the cylinder walls
$Q_м$	kW	175,4	175,4	Heat flux to the oil
$G_{wд}$	kg/s	24,4	24,4	Hot circuit pump capacity
$G_п$	kg/s	0	0	Bypass water flow

Parameter	Dimension	Variants		Description
		1	2	
$G_{вент}$	kg/s	80	80	Airflow through the common fan (fans)
$G_{в1}$	kg/s	62,6	64,3	Fan air flow through R1*
$G_{в2}$	kg/s	15,7	13,9	Fan air flow through R2*
G_{w1}	kg/s	11,1	11,1	Water flow in the cold circuit (through two cold circuit charge air cooler and oil cooler)
G_{w2}	kg/s	24,4	24,4	Water flow through two hot circuit charge air cooler, diesel, and bypass
G_{w12}	kg/s	5,55	5,55	Water flow through one cold circuit charge air cooler
G_{w11}	kg/s	12,2	12,2	Water flow through one hot circuit charge air cooler
$G_{wм}$	kg/s	11,1	11,1	Water flow through the oil cooler
$G_{нв}$	kg/s	5,87	5,87	Supercharging air flow
$G_{м}$	kg/s	14	14	Oil flow
P_1	Pa	500000	500000,0	Air pressure in front of hot circuit charge air cooler
ΔP_1	mm.w.c	149,4	75,5	Air resistance of hot circuit charge air cooler
P_2	Pa	499850,6	499924,5	Air pressure in front of cold circuit charge air cooler
ΔP_2	mm.w.c	354,3	396,8	Air resistance of cold circuit charge air cooler
$T_{в1}$	^oC	34,0	34,0	Air in front of the radiators
$T_1\ (T_к)$	^oC	250,0	250,0	Air behind the compressor
$T_{21}\ (T_{s1})$	^oC	171,5	189,0	Air behind hot circuit charge air cooler
$T_2\ (T_s)$	^oC	54,0	45,0	Air behind cold circuit charge air cooler (in the receiver)
$T_{в12}$	^oC	47,8	49,9	Air behind radiator R1
$T_{в22}$	^oC	89,0	88,5	Air behind radiator R2
$T_{wд1}$	^oC	101,3	100,1	Water in front of the engine
$T_{wд2}$	^oC	105,3	104,0	Water behind the engine
T_{w1}	^oC	41,8	42,7	Water in front of cold circuit charge air cooler
$T_{wм1}$	^oC	56,7	61,0	Water in front of oil cooler
$T_{wм2}$	^oC	60,5	64,7	Water in front of R1 (if there is no bypass)
$T_{wм3}$	^oC	60,5	64,7	Water in front of R1 (for bypass usage)
T_{w3}	^oC	96,8	96,6	Water in front of hot circuit charge air coole
T_{w4}	^oC	101,3	100,1	Water behind hot circuit charge air coole and equal to Twd1
$T_{м1}$	^oC	96,2	96,2	Oil in front of oil cooler (behind the engine)
$T_{м2}$	^oC	90,6	90,2	Oil after oil cooler (in front of the engine)
Hot circuit charge air cooler				
Schema		1	1	Schematic index
b		3	6,00	Number of thermodynamic processes of water
$k_{gнв}$	W/kg·K	263,54	227,61	Mass utilization coefficient
$\eta_{нв1}$		0,51	0,40	Efficiency of hot circuit charge air cooler
$S_{нв}$		0,06	0,06	Specific energy content ratio of coolants on hot circuit charge air cooler

Parameter	Dimension	Variants		Description
		1	2	
$M_{нв}$	kg	8,18	6,64	Mass of hot circuit charge air cooler bundle
Cold circuit charge air cooler				
Schema		1,00	1,00	Schematic index
b		2,00	2,00	Number of thermodynamic processes of water
$k_{gнв}$	W/kg·K	0,00	0,00	Mass utilization coefficient
$\eta_{нв2}$		0,91	0,98	Efficiency of cold circuit charge air cooler
$S_{нв}$		0,02	0,02	Energy consumption ratio of coolants on cold circuit charge air cooler
$M_{нв}$	kg	29,08	58,40	Mass of cold circuit charge air cooler bundle
R1				
Schema		3,00	3,00	Schematic index
b		3,00	3,00	Number of thermodynamic processes of water
$k_{gв1}$	W/kg·K	105,24	105,49	Mass utilization coefficient
$\eta_{р1}$		0,71	0,72	Efficiency of R1
Z1		36,00	37	Number of stands in R1
$M_{р1}$	kg	882,01	906,51	Mass of R1 bundle
R2				
Schema		3,00	3,0	Schematic index
b		1,00	1,0	Number of thermodynamic processes of water
$k_{gв2}$	W/kg·K	117,85	118,7	Mass utilization coefficient
$\eta_{р2}$		0,77	0,8	Efficiency of R2
Z2	pcs	9,00	8,0	Number of stands in R2
$M_{р2}$	kg	220,50	196,0	Mass of R2 bundle
Oil cooler				
Schema		4,00	4,0	Schematic index
b		1,00	1,0	Number of counterflow reversible elements in oil cooler
$k_{gмо}$	W/kg·K	112,27	70,7	Mass utilization coefficient
$\eta_{мо}$		0,14	0,170	Oil cooler efficiency
$S_{м}$		0,66	0,6	Ratio of energy capacities of heat carriers in oil cooler
$M_{мо}$	kg	45,02	82,0	Mass of oil cooler bundle
M_{Σ}	kg	1184,78	1249,6	Mass of all heat exchanger bundles in the system
$\eta_{со}$		0,907	0,949	Cooling system efficiency for intake air

Table 3.4 Results of charge air cooler calculations for EC12A.

Parameter	Dimension	Hot circuit charge air cooler	Cold circuit charge air cooler	Description
$G_в$	kg/s	2,94	2,94	Flow rate of supercharging air
G_w	kg/s	12,20	8,50	Water flow rate
T_1	K	522,95	395,35	Inlet air temperature
T_2	K	461,94	317,80	Outlet air temperature
t_1	^oC	249,95	122,35	Inlet air temperature
t_2	^oC	188,94	44,80	Outlet air temperature
T_{w1}	K	369,32	316,57	Inlet water temperature
T_{w2}	K	461,94	317,80	Outlet water temperature
t_{w1}	^oC	96,32	43,57	Inlet water temperature
t_{w2}	^oC	188,94	44,80	Outlet water temperature
T_{wf}	K	371,08	319,77	Average water temperature
$T_{вf}$	*K*	489,87	337,11	Average air temperature
P_1	Pa	500000	500000	Inlet air pressure
L	m	0,043	0,387	Calculated length of the bundle
B	m	0,3801	0,3801	Calculated width of the bundle
H	m	0,359	0,359	Calculated height of the bundle
$b_{wт}$	pcs	1	6	Thermodynamic number of transverse passages of water
b_w	pcs	1	1	Number of hydraulic passes through water in one thermodynamic cycle
d_w	m	0,00345	0,00345	Height of the tube's cross-section in air
S_1	m	0,00905	0,00905	Distance between tubes in the transverse row
S_2	m	0,0215	0,0215	Pitch between transverse rows of tubes
S_3	m	0,01845	0,01845	Maximum external dimension of the tube's cross-section
S_4	m	0,00172	0,00172	Pitch between fins
$\delta_{ст}$	m	0,0004	0,0004	Tube wall thickness
$\delta_{пл}$	m	0,00006	0,00006	Fin plate thickness
Z_1	pcs	42	42	The largest possible number of tubes in a transverse row
Z_2	pcs	2	18	Number of transverse rows of tubes
Z	pcs	84	756	The number of pipes in the bundle corresponding to the calculated value of the Z_2 number
Heat transfer fluid diagram		1	1	1
F	m^2	6,77	60,9	Fin side surface area
$M_п$	kg	6,66	59,9	Bundle mass
w	m/s	10,24	7,0	Air velocity at the compressed section
w_w	m/s	3,21	1,5	Water velocity in the tubes
$Re_{dэ}$		2790,94	3677,1	Reynolds number for air
Re_w		51677,90	11405,5	Reynolds number for water

Parameter	Dimension	Hot circuit charge air cooler	Cold circuit charge air cooler	Description
k	W/(m^{2}K)	223,85	216,6	Heat transfer coefficient
$\alpha_п$	W/(m^{2}K)	324,08	353,5	Heat transfer coefficient from air to the wall
K_g	W/kgK	227,60	220,3	Bundle mass usage coefficient
K_v	W/m^{3}K	258173,54	249861,2	Bundle volume usage coefficient
Rст	m^2·K/W	6,12E-06	6,12E-06	Thermal resistance of a clean monometallic wall
Rз	m^2·K/W	0,00018	0,000176	Thermal resistance of the contamination layer from the air side
Rw	m^2·K/W	0,00018	0,000176	Thermal resistance of the contamination layer from the water side
R_Σ	m^2·K/W	0,00123	0,001229	Total thermal resistance of a monometallic wall with a contamination layer
η		0,397	0,984	Coefficient of useful action of the supercharging air cooler
ΔP	Pa	740,01	3889,05	Air resistance of the bundle
ΔP	mm.w.c	75,51	396,84	Air resistance of the bundle
ΔP_w	kPa	22,14	29,76	Bundle resistance in water
ρ*		1,13	1,23	Degree of increase in air density in the bundle
Q	kW	179,95	228,76	Heat flow into the water

Table 3.5 Results of oil cooler calculations for EC12A.

Parameter	Dimension	Oil cooler	Description
G	kg/s	14	Oil flow rate
$t_{м1}$	°C	96,21	Inlet oil temperature
$p_{м1}$	kPa	439	Inlet oil pressure
$t_{м2}$	°C	90,22	Outlet oil temperature
η		0,170	Oil cooler efficiency
$w_м$	m/s	0,49	Average oil velocity at the compressed section
ΔPм	kPa	9,35	Oil resistance
G_w	kg/s	11,10	Water flow rate
t_{w1}	°C	60,96	Temperature of water at the inlet
t_{w2}	°C	64,74	Temperature of water at the outlet
P_w	kPa	180	Pressure of water at the inlet
w_w	m/s	1,75	Velocity of water at the compressed section
ΔPw	kPa	15,01	Resistance by water
$R_{ст}$	m^2·K/W	0,00240	Total resistance of the wall and contamination layer
k_g	W/kgK	70,7	Coefficient of mass utilization of the bundle
Q	kW	175,8	Heat flow into the water

Parameter	Dimension	Oil cooler	Description
Type of heat exchange surface		Monometallic	Monometallic
D	m	0,0245	Fin diameter
d_o	m	0,0125	Diameter of the supporting tube
d_1	m	0,0118	For bimetallic material
d_w	m	0,01	Internal diameter of the tube
u	m	0,002	Pitch between fins
δ_1	m	0,00055	Thickness of the fin at the edge
δ_2	m	0,0002	Thickness of the fin at the base
S_1	m	0,027	Transverse pitch of tubes in the bundle
S_2	m	0,0234	Longitudinal pitch of tubes in the bundle
Scheme		4	Symbol for the mutual flow pattern; 4 – reverse current.
b		1	Total number of counterflow-connected reversible elements
$b_м$		3	Number of strokes for oil
b_w		2	Number of strokes for water
$S_д$	m	0,005	Thickness of the diaphragm
$Z_д$		17	Actual number of tubes in the second row from the center
Z_2		11	Number of transverse rows of tubes between diaphragm cutouts
Zcv		0	Number of tubes in the diaphragm cutout
Z		166	Total number of tubes in the bundle
$H_{ст}$	m	0,119	Height of the segment cutout
Dо	m	0,459	Diameter of the circle circumscribed around the bundle cross-section
$D_т$	m	0,496	Internal diameter of the housing
$D_{ду}$	m	0,496	Diameter of the flexible seal assembly with the housing
$\delta_д$	m	0,0005	Clearance on the side between the tube and the diaphragm
Lп	m	0,259	Depth of the tube bundle
$Z_{дф}$		2	Number of diaphragms
k_D		0,4	Ratio of the length of the middle compartment to the internal diameter of the housing
L_1	m	0,1688	Length of the middle compartment
L_2	m	0,1688	Length of the compartment with oil supply
L_3	m	0,1688	Length of the compartment with oil discharge
Lт	m	0,5163	Length of the heat exchanger tubes taking into account shading by diaphragms
$D_{пw}$	mm	83	Internal diameter of the water inlet pipe
$D_{опw}$	mm	83	Internal diameter of the water outlet pipe

Parameter	Dimension	Oil cooler	Description
$D_п$	mm	100	Internal diameter of the oil inlet pipe
$D_{оп}$	mm	100	Internal diameter of the oil outlet pipe
Мп	kg	83,57	Mass of the tube bundle
F	m^2	33,02	Total surface area for heat exchange on the fin side
		Right	Indicator of correct program operation

Table 3.6 Results of Radiators Calculations for EC12A.*

.

Parameter	Dimension	R1	R2	Description
$G_в$	kg/s	1,739	1,739	Air flow rate
G_w	kg/s	0,3	3,050	Water flow rate
$T_{в1}$	К	307	307,0	Air temperature before the radiator
$T_{в2}$	К	322,9	361,5	Air temperature after the radiator
$t_{в1}$	^oC	34	34,0	Air temperature before the radiator
t_2	^oC	49,9	88,5	Air temperature after the radiator
T_{w1}	К	337,7	377,04	Water temperature before the radiator
T_{w2}	К	315,7	369,58	Water temperature after the radiator
t_{w1}	^oC	64,7	104,04	Water temperature before the radiator
t_{w2}	^oC	42,7	96,6	Water temperature after the radiator
P_1	Pa	100000	100000	Air pressure before the radiator
$L_п$	m	0,209	0,209	Depth of the radiator bundle in the direction of airflow
$B_п$	m	0,1474	0,1474	Radiator bundle width
$H_п$	m	1,206	1,206	Radiator bundle height
$b_{w\Sigma}$		6	1	Total number of cross-flows of water
$b_{wт}$		3	1	Number of thermodynamic flows of water in the radiator
b_w		2	1	Number of hydraulic paths of water in one thermodynamic paths
d_w	m	0,0025	0,0025	Cross-sectional height of the tube
S_1	m	0,0134	0,0134	Spacing between tubes in the transverse row
S_2	m	0,019	0,019	Pitch between transverse rows of tubes
S_3	m	0,017	0,017	Largest dimension of the tube cross-section
S_4	m	0,0023	0,0023	Pitch between fins
$\delta_{ст}$	m	0,00025	0,00025	Tube wall thickness
$\delta_{пл}$	m	0,0001	0,0001	Thickness of the fin plate
$h_г$	m	0,0005	0,0005	Height of the corrugation from the surface

Parameter	Dimension	R1	R2	Description
e	m	0,0015	0,0015	Convexity diameter
$Z_{2г}$	pcs	5	5	Number of transverse rows of corrugations between tubes
$Z_{1г}$	pcs	2	2	The greatest number of corrugations between tubes in a transverse row along the air flow
$S_{г1}$	m	0,0079	0,0079	Pitch between longitudinal rows of corrugations
$S_{г2}$	m	0,00388	0,0039	Actual pitch between transverse rows of corrugations
i	pcs	8	8	Number of corrugations on the edge between two adjacent tubes
Z_1	pcs	11	11	Maximum possible number of tubes in a transverse row
Z_2	pcs	11	11	Number of transverse rows of tubes
Z	pcs	116	116	Number of tubes in the bundle corresponding to the calculated value of Z_2
Coolant flow diagram		3	3	3 – cross current, both coolants do not mix
F	m^2	33,1	33,1	Surface area on the fin side
$M_п$	kg	24,5	24,500	Bundle mass
T_{wf}	К	326,7	373,3	Average water temperature in the radiator
$T_{вf}$	К	310,3	320,91	Average air temperature in the radiator
w_w	m/s	0,5	0,82	Water velocity in the tubes
Re_w		3211,5	10435,5	Reynolds number for water
Re		1685,8	1641,1	Reynolds number for air
R_Σ	$(m^2К)/W$	0,0013	1,29E-03	Total thermal resistance of the fouled heat exchange surface
ΔP	mm.w.c	49,4	49,4	Air resistance of the radiator
ΔP_w	kPa	11,6	4,4	Resistance of the radiator in terms of water
k	$W/(m^2К)$	78,0	87,8	Heat transfer coefficient
Kg	W/kgК	105,5	118,662	Mass flow utilization coefficient
K_v	$W/m^3К$	69561,91	78251,03	Volume flow utilization coefficient
η		0,717	0,7780	Radiator thermal efficiency
ΔLr_c	J/kg	378,2	420,67	Gas dynamic losses in the section
ρ_2	kg/m^3	1,075	0,9595	Air density in the shaft

*Note:

Calculations are performed for one stand of each radiator. In this case, the values ΔP, ΔP_w, η and some others coincide with the data for the entire radiator.

Answers to Computational Questions

The potential rational limit of the coolant temperatures provided by the system while adhering to all accepted constraints is given in Table 3.3, Variant 1. Variant 2 presents the calculation results when increasing the dimensions of the charge air cooler against the established limitations. Tables 3.4, 3.5, and 3.6 provide the calculation results for all heat exchangers for Variant 2. In principle, the parameters of the heat exchangers can be improved, which is a further design task for manufacturing. In particular, it is possible to reduce the excessive water velocities in the tubes of the hot circuit charge air cooler by introducing a bypass for part of the water. To achieve a rational oil cooler design, a bypass for water should be introduced bypassing the oil cooler, as shown in the diagram.

In Variant 1, all accepted constraints are observed. In Variant 2, the constraints on the dimensions of the charge air cooler front are violated.

Answer to Question№1 for Variant №1

The values of the control temperatures of water and oil are close to the specified ones. The system can achieve the desired temperatures of water and oil.

The air temperature in the receiver (T_s) is higher than the specified value and is 54°C against the specified 45°C. The system cannot provide the specified air temperature in the receiver.

The water temperature after the engine is 105.3°C, which is 2.7 K below the assigned temperature (108°C). Temperature control by the number of transverse rows of tubes in hot circuit charge air cooler and the number of posts in the radiator blocks leads to discrete changes in temperature since the numbers of rows of tubes and the number of posts cannot be fractional. As a result, the water temperature after the engine is either lower or higher than the assigned value. Introducing a bypass for water around hot circuit charge air cooler can precisely set this temperature.

The oil temperature after the engine is 0.2 K above the specified value.

The air resistance of the charge air cooler block is almost equal to the permissible limit.

The resistances for water and oil in all heat exchangers are within permissible limits.

The water velocities in the tubes of hot circuit charge air cooler are higher than permissible, but this can be corrected by introducing a bypass for water around hot circuit charge air cooler in the system and making some changes in other heat ex

changers. For other heat exchangers, this parameter is within the norm.

The temperature differences between water and oil on the engine are 3.9 K and 5.7 K, respectively, which complies with existing norms and the specified initial data.

Thus, the temperatures of water and oil after the engine are sufficiently close to the desirable values, while the air temperature is 9 K higher.

Answer to Question №1 for Variant№2.

With an increase in the dimensions of the charge air cooler bundle front to the dimensions of the housing, it is possible to achieve the desired value of T_s = 45°C while maintaining the limit on the air resistance of the bundle.

The total number of radiator posts remains unchanged. The airflow does not change.

The efficiency of hot circuit charge air cooler in this variant will be reduced (due to a decrease in the length of the bundle), and the efficiency of cold circuit charge air cooler will increase.

The number of posts in radiator R1 needs to be increased, and in radiator R2 decreased, while keeping the total number of posts unchanged.

The design and parameters of the oil cooler need to be changed. The overall mass of the heat exchanger cores in the system increases slightly.

The temperatures of other coolants are close to the desirable values. The water temperature after the engine can precisely correspond to 108°C if a bypass for water around hot circuit charge air cooler is used (not considered in the results).

Answer to Question №2 for Variant №1

The temperature of the air in the receiver can be lowered mainly in two ways: increase the efficiency of cold circuit charge air cooler and/or increase the cooling air flow.

It is most effective to increase the efficiency of cold circuit charge air cooler (effective if the efficiency of charge air cooler is less than 0.97).

The efficiency of cooling the intake air will also increase with an increase in the cooling air flow rate (this method is secondary and effective at low efficiency of the radiator block operating on charge air cooler). Increasing $G_в$ is almost impossible without simultaneously increasing the total number of radiator posts Z_c since the air resistance of the posts should not significantly increase.

Increasing the efficiency of cold circuit charge air cooler is possible by increasing the depth of the bundle (the established limit of the bundle length in the calculations is far from reached) and by increasing the size of its front. In this case, efficiency increases while maintaining acceptable air resistance.

Increasing the size of the charge air cooler front violates the established restrictions on the dimensions of the charge air cooler block.

Increasing the cooling air flow rate $G_в$, as well as increasing the total number Z_c in this case, will lead to a violation of the restrictions adopted based on a comparison of the considered system with a competitive one.

For the sake of compactness of the cooling system, it is desirable to have a high temperature of water behind the engine (in Kolomna, for similar installations, this temperature is 108°C), but not exceeding a certain limit, as an increase in temperature is associated with a decrease in the efficiency of the engine itself.

The temperature of the water behind the engine can be regulated by changing the efficiency of hot circuit charge air cooler (increasing efficiency raises the temperature of the water behind the engine), changing the number of radiator struts in block R2 (reducing the number of struts increases the water temperature), and introducing a bypass for water around hot circuit charge air cooler. The first two methods provide discrete temperature control. Precise and smooth temperature control is achieved by simultaneously using all three methods.

Thus, for the precise establishment of the designated temperature of the water behind the engine, a minor correction of the scheme is sufficient. To establish the designated temperature of the air in the receiver, it would be necessary either to violate the specified restrictions on the dimensions of the charge air cooler bundle front or to increase the cooling air flow rate and the total number of radiator struts against the corresponding parameters of a potential competitor.

Answer to Question №2 for Variant №2.

In principle, there are reserves for improving parameters. In particular, further lowering the temperature of the air in the receiver can be achieved by the same methods outlined above in **variant** №1.

Answer to Question №3 for Variant №1

The efficiency of this system for cooling the supercharged air, taking into account the specified limitations, is 0.907, which is a very high value. However, the desired temperature in the engine's receiver is not achieved under the specified initial conditions and accepted limitations.

The mass of the heat exchanger cores is approximately 1187 kg, which corresponds to approximately 0.49 kg/kW. The latter is a good indicator.

At the same time, the efficiency of cooling the air in the hot circuit is very low, and a two-circuit heat exchanger is complex. The use of two circuits and two pumps complicates the system.

Answer to Question №3 for Variant №2.

This variant of the cooling system already provides η_o = 0.95, which is a very good indicator and has fundamental possibilities for improvement (with a violation of the accepted limitations).

The mass of the heat exchanger cores is 1250 kg, which corresponds to 0.52 kg/kW. The latter is a good indicator but worse than for the previous option.

The efficiency of cooling the air in the hot circuit is very low, and a two-circuit heat exchanger is complex. The use of two circuits and two pumps complicates the system.

Answer to Question №4 for Variant №1.

Partially, the answers to this question have been provided above. The choice of the most efficient solutions was made based on a series of variant calculations. As a result, the following was established.

The most effective way to lower the air temperature in the receiver would be to increase the dimensions of the heat exchanger, specifically, the frontal area of the bundle. Simultaneously with changing the dimensions of the heat exchanger, the parameters of other heat exchangers should be adjusted to achieve the designated temperatures of water and oil behind the engine.

The total number of radiator struts and the flow rate of cooling air can remain unchanged.

Answer to Question №4 for Variant №2.

The system approximately provides all designated temperatures. To achieve an exact match of the water temperature behind the engine, it is advisable to introduce a bypass around hot circuit charge air cooler.

While adhering to all accepted constraints, the EC12A -type system ensures water and oil temperatures behind the engine that are close to the designated values. An exact match of these temperatures with the designated ones is possible by introducing bypasses for water around hot circuit charge air cooler and oil cooler into the scheme. The specified air temperature in the receiver is not provided.

The required air temperature in the receiver can be achieved if the dimensions of the charge air cooler frontal area slightly exceed the specified limitations. In this case, other heat exchangers in the system should also be modified without violating the accepted constraints.

Thus, the system is effective in cooling water, oil, and charge air. However, it has the following drawbacks:

- Cooling in the hot circuit is inefficient.
- The complex charge air cooler is structurally complicated.
- Two pumps and two circuits complicate the system.

The cooling system can be simplified and its mass reduced under other equal conditions. To achieve this, it is possible to transition to a more modern system scheme. A more modern system (2PK1M) is presented below.

3.4 Low-Flow System Design 2PK1M .

For the engine 12FC18,5/21,5, a two-radiator single-pump low-flow system (designated as 2PK1M) has been developed to simplify the system and reduce its mass under otherwise equal conditions. The term 'low-flow' is used because the flow of water through the heat exchanger (charge air cooler) is much lower than in conventional, full-flow systems, where it is typically assumed to be equal to the pump flow rate.

3.5 Cooling System Design Scheme.

The system diagram is presented in Figure 3.3.

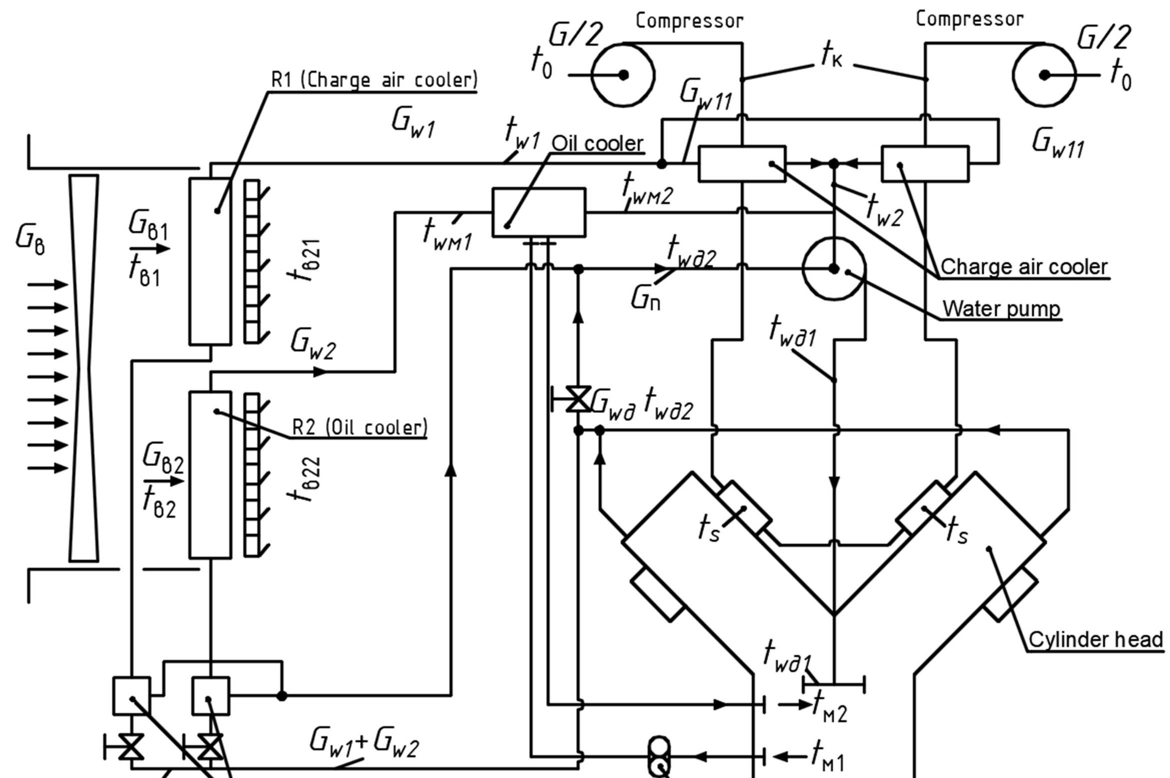

Figure 3.3 – Diagram of the two-radiator low-flow cooling system type 2PK1M.

It is assumed that a common fan (or fans) is used for both radiators, and the air is distributed proportionally to the number of partitions across the radiator blocks.

In the operation of this cooling system, one portion of the fresh water flow, $G_{wд}$ (usually the larger portion), exiting the engine without any cooling, passes through the bypass to the suction of the circulation pump in the amount of $G_{wп}$. The second portion (usually the smaller part, $G_{w1} + G_{w2}$) is directed in parallel to two cooling blocks: R1 and R2. In these coolers (radiators), fresh water is cooled by fan air with flows $G_{в1}$ and $G_{в2}$.

After passing through the radiators, the cooled fresh water enters the inlets of the heat exchanger (charge air cooler) and oil cooler (oil cooler), cooling the charge air and oil. The water flows exiting the heat exchanger and oil cooler then proceed to the pump inlet, where they are mixed with water from the bypass. After mixing, the water enters the engine. The blending of water flows ensures the required temperature at the engine inlet, $t_{wд1}$.

The water flows through the circuits, R1- charge air cooler and R2- oil cooler, are optimized during the system calculation, and the corresponding values are set during system tuning using throttles in front of the radiators. The low water flow through R1 allows for high efficiency of this cooler block with relatively small dimensions, resulting in the fresh water after R1 having a temperature close to the ambient air temperature at the inlet to R1. The design of R1 as a block with standard partitions, each of which has multiple passages for fresh water (for this, the head of the partitions must have a special design), contributes to achieving high efficiency of the entire block. The heat exchanger (charge air cooler) is designed in a multiple cross-flow scheme with a common counterflow, allowing for high efficiency with the necessary compactness and acceptable water resistance. The efficiency of the charge air cooler is practically the same as for full-flow constructions.

The transition to a larger number of passages contributes to the increase in efficiency. The reduction in water velocity, associated with the need to maintain acceptable water resistance, leads to a decrease in the heat transfer coefficient and a decrease in efficiency. These two opposing factors ultimately balance each other out.

The low water temperature at the inlet to the charge air cooler and the high efficiency of charge air cooler ensure a low air temperature in the engine receiver, which is the main advantage of low-flow cooling systems.

Similarly, the second branch of the cooling system, consisting of block R2 and oil cooler, operates. When organizing the water flow through this branch and selecting the efficiency of the heat exchangers included in it, it is considered that the system does not require an extremely low oil temperature. Consequently, the efficiency of oil cooler will be lower than the efficiency of circuit charge air cooler.

In addition, when designing the system, it is necessary to consider that both cooler blocks dissipate not only the heat from the charge air and oil but also the heat generated into the water in the engine's cooling space. As a result, the efficiency of all heat exchangers in the system, water flows through them, and through the bypass, are selected considering both the desired temperatures of all heat carriers and the heat flows generated by the cooling system. This also takes into account the possible minimization of the total mass of heat exchange elements of all heat exchangers in the system.

At partial loads and during a decrease in ambient temperature, the system regulates the temperatures of charge air, oil, and water. Thermal regulation is achieved by adjusting the flow of fan air through the radiators and the operation of thermostats in the fresh water circuit, diverting water bypassing the radiators to the pump inlet. By changing the flows of fan air and water through the radiators, it is possible to regulate not only the depth of cooling but also to provide heating of the charge air and oil at low loads and in colder ambient temperatures.

The calculations for this system were performed using the calculation complexes described above. The results of the system calculations are presented in tabular form slightly below. Calculations are provided for two variants with temperatures t_s equal to analogous values for the EC12A system.

Oil and water temperatures after the engine are precisely maintained within specified limits (108 and 96°C).

To assess the parameters of the proposed system, especially to evaluate the possibility of achieving the specified control temperatures ($t_{wд2}$ = 108 °C, $t_{м1}$ = 96 °C и t_s =45°C), numerous preliminary calculations were conducted. Based on these calculations, it was determined that the specified control temperatures could be achieved with reduced cooling air flow ($G_в$ = 60 kg/s compared to 80 kg/s in the EC12A system) and a reduction in the total number of radiator partitions from 46 to 32.

3.6 Analysis of the obtained results.

In Table 3.7, two results of calculations for the 2PK1M system are presented.

In Option 1, the dimensions of the charge air cooler are maintained according to the BerMP requirements. As a result, the same air temperature in the receiver (54°C) is obtained as in the EC12A system. At the same time, a water temperature of 108°C behind the engine and oil temperature of 96°C are ensured. With practically the same temperatures of the heat carriers as in the EC12A system, the 2PK1M system has a smaller number of radiator posts (32 versus 46), lower cooling air consumption (60 kg/s versus 80 kg/s), and a smaller total core mass of heat exchangers (904 kg versus 1184 kg). Accordingly, the specific mass of the system (core mass/engine power) is 0.4 kg/kW, which is less than that for EC12A. The system has one pump, one circuit, and the charge air cooler is not divided (there is no hot and cold part of the bundle). The system is simpler, lighter, and requires less water and air for operation. Less energy is expended to pump water and air in the system's operation.

The calculation results for all heat exchangers are presented in tables 3.8, 3.9, and 3.10 under № 1.

In Option 2, the dimensions of the charge air cooler are increased (up to the same limits as in the EC12A system). After that, the water flows in the branches of the system have been slightly changed. The efficiency and the design of the oil cooler have changed. The total number of radiator posts and the cooling air consumption remain the same. The air temperature in the receiver has dropped to the specified BerMP value of 45°C. At the same time, the water and oil temperatures behind the engine are maintained at the same values as in Option 1 (108 and 96°C). The calculation results for all heat exchangers are presented in tables 3.8, 3.9, and 3.10 under №2.

In this case, the mass of the heat exchanger cores increases by approximately 50 kg (calculated as 962 kg versus 904 kg). In the EC12A system, the sum of the core masses for the increased charge air cooler increases by approximately the same amount – from 1185 kg to 1249 kg. The mass of the heat exchanger cores in the first option for 2PK1M is less than that for EC12A, by 280 kg, and in the second option, it is less by 292 kg.

Table 3.7 Results of the calculation for the 2PK1M system.

Parameter	**Dimension**	**Variants**		**Description**
		1	**2**	
$Q_д$	kW	403	403	Heat flux to the cylinder walls
$Q_м$	kW	175,0	175,0	Heat flux to the oil
$G_в$	kg/s	60,0	60,0	Fan air flow
$G_{в1}$	kg/s	41,3	41,25	Air flow rate through radiator R1 (charge air cooler)
$G_{в2}$	kg/s	16,9	16,9	Air flow rate through radiator R2 (oil cooler)
G_{w1}	kg/s	4,245	4,511	Water flow rate through charge air cooler
G_{w2}	kg/s	2,00	2,00	Water flow rate through oil cooler
$G_{wп}$	kg/s	18,2	17,9	Water flow rate through bypass
G_w	kg/s	24,4	24,4	Water flow rate through diesel engine
$G_{нв}$	kg/s	5,87	5,9	Supercharging air flow
$G_м$	kg/s	14	14	Oil flow
Zc .	pcs	32	32	Total number of radiator sections
Z_1	pcs	22	22	Number of radiator sections R1
Z_2	pcs	9	9	Number of radiator sections R2
$Z_г$	pcs	1	1	Number of radiator sections for hydraulics
Mc	kg	24,50	24,50	Mass of one radiator section

Parameter	Dimension	Variants		Description
		1	2	
P_1	Pa	500000,00	500000,00	Air pressure after the compressor
$T_{в1}$	K	34,00	34	Air before the compressor
T_0	K	34,00	34,00	Air before the radiator
$T_1\ (T_к)$	K	250,00	250,00	T1 or Tk, air after the compressor
$T_2\ (T_s)$	K	54,01	44,94	T2 or Ts, air after the intercooler
$T_{в21}$	K	62,82	64,11	Air after the intercooler radiator
$T_{в22}$	K	65,81	65,81	Air after the oil cooler radiator
$T_{wд1}$	K	104,06	104,06	Water before the diesel engine
$T_{wд2}$	K	108,00	108,00	Temperature of water after the engine
T_{w1}	K	40,83	41,96	Water before the intercooler
T_{w2}	K	105,83	105,96	Water after the intercooler
$T_{wм1}$	K	43,62	43,62	Water before the oil cooler
$T_{wм2}$	K	64,51	64,51	Water after the oil cooler
$T_{м1}$	K	96,00	96,00	Oil at the engine outlet or at the oil cooler inlet
$T_{м2}$	K	89,93	89,93	Oil after the oil cooler
Charge air cooler				
Schema		1	1	Schematic index
b		10	10	Number of thermodynamic processes of water
$k_{gнв}$	W/kg·K	323,7	253,6	Mass utilization coefficient
$\eta_{нв}$		0,937	0,986	Efficiency of charge air cooler
$\Delta p_{нв}$	mm.w.c.	446,2	510,0	Air resistance
$\Delta p_{wнв}$	kPa	13,4	6,64	Water resistance
$S_{нв}$		0,332	0,312	Energy consumption ratio on the charge air cooler
$M_{нв}$	kg	65,7	133,1	Charge air cooler bundle mass
R_1				
Schema		3	3	Schematic index
b		5	5	Number of thermodynamic processes of water
$k_{gр}$	W/kg·K	113,83	114,9	Mass utilization coefficient
$\eta_{р1}$		0,908	0,892	Efficiency of R1
Δp_1	mm.w.c.	55,9	55,93	Air resistance
Δp_{w1}	kPa	23,0	25,63	Water resistance
$S_{р1}$		0,4	0,46	Energy consumption ratio on the radiator
Z1	pcs	22	22,00	Number of stands in R2

Parameter	**Dimension**	**Variants**		**Description**
		1	**2**	
M_{p1}		539	539,0	Mass of R2 bundle
R_2				
Schema		3	3	Schematic index
b		5	5	Number of thermodynamic processes of water
k_{gp}	W/kg·K	116,1	116,1	Mass utilization coefficient
η_{p2}		0,870	0,870	Efficiency of R2
Δp_2	mm.w.c.	55,99	56,0	Air resistance
Δp_{w2}	kPa	29,56	29,6	Water resistance
S_{p2}		0,494	0,49	Energy consumption ratio on the radiator
Z2	pcs	9	9,00	Number of stands in R2
M_{p2}	kg	220,5	220,50	Mass of R2 bundle
Oil cooler				
Schema		4	4	Schematic index
b		2	2	Number of counterflow reversible elements in oil cooler
$k_{gмо}$	W/kg·K	76,244	76,2	Mass utilization coefficient
$\eta_{мо}$		0,404	0,404	Oil cooler efficiency
$\Delta p_{м}$	kPa	29,6	29,6	Total resistance for oil of all units
$\Delta p_{wм}$	kPa	33,6	33,6	Total resistance for water of all units
$S_{м}$		0,291	0,29	Ratio of energy capacities of heat carriers in oil cooler
$M_{мо}$	kg	59,9	59,9	Mass of oil cooler bundle
$\eta_{о}$		0,907	0,949	Cooling system efficiency for intake air
M_{Σ}	kg	885,1	952,6	Mass of all heat exchanger bundles in the system

Table 3.8 Results of charge air cooler calculations for 2RK1M.

Parameter	**Dimension**	**Variants**		**Description**
		1	**2**	
$G_{в}$	kg/s	2,94	2,94	Flow rate of supercharging air
G_{w}	kg/s	2,12	2,26	Water flow rate

Parameter	Dimension	Variants		Description
		1	2	
T_1	K	523,0	523,0	Inlet air temperature
T_2	K	327,0	317,9	Outlet air temperature
t_1	°C	250,0	250,0	Inlet air temperature
t_2	°C	54,01	44,94	Outlet air temperature
T_{w1}	K	313,8	315,0	Inlet water temperature
T_{w2}	K	327,0	317,9	Outlet water temperature
t_{w1}	°C	40,8	42,0	Inlet water temperature
t_{w2}	°C	54,0	44,9	Outlet water temperature
T_{wf}	K	345,3	346,0	Average water temperature
$T_{вf}$	K	399,7	381,8	Average air temperature
P_1	Pa	500000	500000	Inlet air pressure
L	m	0,258	0,43	Calculated length of the bundle
B	m	0,362	0,3801	Calculated width of the bundle
H	m	0,31	0,359	Calculated height of the bundle
$b_{wт}$	pcs	10	10	Thermodynamic number of transverse passages of water
$b_{wг}$	pcs	1	1	Number of hydraulic passes through water in one thermodynamic cycle
d_w	m	0,00345	0,00345	Height of the tube's cross-section in air
S_1	m	0,00905	0,00905	Distance between tubes in the transverse row
S_2	m	0,0215	0,0215	Pitch between transverse rows of tubes
S_3	m	0,01845	0,01845	Maximum external dimension of the tube's cross-section
S_4	m	0,00172	0,00172	Pitch between fins
$\delta_{ст}$	m	0,0004	0,0004	Tube wall thickness
$\delta_{пл}$	m	0,00006	0,00006	Fin plate thickness
Z_2	pcs	12	20	Number of transverse rows of tubes
Z_1	pcs	40	42	Number of longitudinal rows of tubes (number of tubes in one transverse row)
Z	pcs	480	840	Number of tubes in a bundle
Heat transfer fluid diagram		1	1	1
F	m^2	33,4	67,7	Bundle area from the air side
$M_п$	kg	32,8	66,6	Bundle mass
w	m/s	10,2	8,0	Air velocity at the compressed section
w_w	m/s	1,0	0,6	Water velocity in the tubes

Parameter	Dimension	Variants		Description
		1	2	
$Re_{dэ}$		3924,4	3340,3	Reynolds number for air
Re_w		11231,0	6884,1	Reynolds number for water
k	W/(m^{2}K)	318,3	249,4	Heat transfer coefficient
$\alpha_п$	W/(m^{2}K)	438,3	357,2	Heat transfer coefficient from air to the wall
K_g	W/kgK	323,7	253,6	Bundle mass usage coefficient
K_v	W/m^{3}K	367129,0	287666,3	Bundle volume usage coefficient
Rст	m^2·K/W	0,000006	0,000006	Thermal resistance of a clean monometallic wall
Rз	m^2·K/W	1,76E-04	1,76E-04	Thermal resistance of the contamination layer from the air side
Rw	m^2·K/W	1,76E-04	1,76E-04	Thermal resistance of the contamination layer from the water side
R_Σ	m^2·K/W	3,00E-04	3,00E-04	Total thermal resistance of a monometallic wall with a contamination layer
η		9,37E-01	9,86E-01	Coefficient of useful action of the supercharging air cooler
ΔP	Pa	4373,1	4997,8	Air resistance of the bundle
ΔP	mm.w.c	446,23	509,98	Air resistance of the bundle
ΔPw	kPa	13,4	6,6	Bundle resistance in water
ρ*		1,585	1,629	Degree of increase in air density in the bundle
Q	kW	578,1	604,9	Heat flow into the water

Table 3.9 Results of oil cooler calculations for 2RK1M.

Parameter	Dimension	Variants	Oil cooler 2	Description
G	kg/s	14	14	Oil flow rate
$t_{м1}$	°C	96	96	Inlet oil temperature
$p_{м1}$	kPa	439	439	Inlet oil pressure
$t_{м2}$	°C	89,93	89,93	Outlet oil temperature
η		0,404	0,404	Oil cooler efficiency
$w_м$	m/s	1,25	1,25	Average oil velocity at the compressed section
ΔPм	kPa	29,56	29,56	Oil resistance
G_w	kg/s	2,00	2,00	Water flow rate
t_{w1}	°C	43,62198	43,6	Temperature of water at the inlet

Parameter	Dimension	Variants	Oil cooler 2	Description
		579		
t_{w2}	^{o}C	64,81	64,81	Temperature of water at the outlet
P_w	kPa	180	180	Pressure of water at the inlet
w_w	m/s	1,50	1,50	Velocity of water at the compressed section
ΔPw	kPa	33,61	33,61	Resistance by water
$R_{ст}$	$m^2 \cdot K/W$	0,00243	0,00243	Total resistance of the wall and contamination layer
k_g	W/kgK	76,2	76,2	Coefficient of mass utilization of the bundle
Q	kW	177,5324 9	177,5	Heat flow into the water
Type of heat exchange surface		monome-tallic	monometallic	Type of roller pipes
D	m	0,0245	0,0245	Fin diameter
d_o	m	0,0125	0,0125	Diameter of the supporting tube
d_1	m	0,0118	0,0118	For bimetallic material
d_w	m	0,01	0,01	Internal diameter of the tube
u	m	0,002	0,002	Pitch between fins
δ_1	m	0,00055	0,00055	Thickness of the fin at the edge
δ_2	m	0,0002	0,0002	Thickness of the fin at the base
S_1	m	0,027	0,027	Transverse pitch of tubes in the bundle
S_2	m	0,0234	0,0234	Longitudinal pitch of tubes in the bundle
Scheme		4	4	Symbol of mutual flow pattern; 4 – reverse current.
b		1	1	Total number of counterflow-connected reversible elements
$b_м$		7	7	Number of strokes for oil
b_w		6	6	Number of strokes for water
$S_д$	m	0,005	0,005	Thickness of the diaphragm
$Z_д$		13	13	Actual number of tubes in the second row from the center
Z_2		9	9	Number of transverse rows of tubes between dia-phragm cutouts
Zcv		0	0	Number of tubes in the diaphragm cutout
Z		104	104	Total number of tubes in the bundle
$H_{ст}$	m	0,084	0,084	Height of the segment cutout
Do	m	0,352	0,352	Diameter of the circle circumscribed around the bun-dle cross-section
$D_т$	m	0,380	0,380	Internal diameter of the housing
$D_{ду}$	m	0,380	0,380	Diameter of the flexible seal assembly with the hous-ing

Parameter	Dimension	Variants	Oil cooler 2	Description
$\delta_д$	m	0,000500	0,0005	Clearance on the side between the tube and the diaphragm
$L_П$	m	0,212	0,212	Depth of the tube bundle
$Z_{дф}$		6	6	Number of diaphragms
k_D		0,25	0,25	Ratio of the length of the middle compartment to the internal diameter of the housing
L_1	m	0,086	0,086	Length of the middle compartment
L_2	m	0,094	0,095	Length of the compartment with oil supply
L_3	m	0,094	0,095	Length of the compartment with oil discharge
$L_Т$	m	0,649	0,650	Length of the heat exchanger tubes taking into account shading by diaphragms
$D_{пw}$	mm	83	83	Internal diameter of the water inlet pipe
$D_{опw}$	mm	83	83	Internal diameter of the water outlet pipe
$D_п$	mm	100	100	Internal diameter of the oil inlet pipe
$D_{оп}$	mm	100	100	Internal diameter of the oil outlet pipe
$М_П$	kg	65,9	65,9	Mass of the tube bundle
F	m^2	26,03	26,03	Total surface area for heat exchange on the fin side

Table 3.10 Results of Radiators Calculations for 2RK1M.*

	Dimension	Variants			
		1	2	1	2
		R1	R1	R2	R2
$G_в$	kg/s	1,88	1,88	1,9	1,9
G_w	kg/s	0,19	0,21	0,22	0,22
$T_{в1}$	K	307	307	307,0	307,0
$T_{в2}$	K	335,8	337,1	338,8	338,8
$t_{в1}$	°C	34	34	34,0	34,0
t_2	°C	62,8	64,1	65,8	65,8
T_{w1}	K	381	381	381,0	381,0
T_{w2}	K	313,8	315,0	316,6	316,6
t_{w1}	°C	108	108	108,0	108,0
t_{w2}	°C	40,8	42,0	43,6	43,6
P_1	Pa	100000	100000	100000,0	100000,0
$L_п$	m	0,209	0,209	0,209	0,209
$B_п$	m	0,1474	0,1474	0,1474	0,1474
$H_п$	m	1,206	1,206	1,206	1,206
$b_{w\Sigma}$		10	10	10,0	10,0

	Dimension	Variants			
		1	2	1	2
		R1	**R1**	**R2**	**R2**
$b_{wт}$		5	5	5,0000	5,0000
b_w		2	2	2,0000	2,0000
d_w	m	0,0025	0,0025	0,0025	0,0025
S_1	m	0,0134	0,0134	0,0134	0,0134
S_2	m	0,019	0,019	0,0190	0,0190
S_3	m	0,017	0,017	0,0170	0,0170
S_4	m	0,0023	0,0023	0,0023	0,0023
$\delta_{ст}$	m	0,00025	0,00025	0,0003	0,0003
$\delta_{пл}$	m	0,0001	0,0001	0,0001	0,0001
$h_г$	m	0,0005	0,0005	0,0005	0,0005
e	m	0,0015	0,0015	0,0015	0,0015
$Z_{2г}$	pcs	5	5	5,0	5,0
$Z_{1г}$	pcs	2	2	2,0	2,0
$S_{Г1}$	m	0,0079	0,0079	0,008	0,008
$S_{Г2}$	m	0,0039	0,0039	0,004	0,004
i	pcs	8	8	8,0	8,0
Z_1	pcs	11	11	11,0	11,0
Z_2	pcs	11	11	11,0	11,0
Z	pcs	116	116	116,0	116,0
Flow scheme of coolants		3	3	3	3
F	m^2	33,11	33,11	33,1	33,1
$M_п$	kg	24,50	24,50	24,5	24,5
T_{wf}	K	347,42	347,98	348,8	348,8
$T_{вf}$	K	327,94	327,82	327,7	327,7
w_w	m/s	0,52	0,55	0,6	0,6
Re_w		4728,1	5064,2	5552,5	5552,5
Re		2384,7	2385,4	2385,9	2385,9
R_Σ	$(m^2K)/W$	0,00129	0,00129	0,0013	0,0013
ΔP	mm.w.c	55,9	55,9	56,0	56,0
ΔP_w	kPa	23,0	25,6	29,6	29,6
k	$W/(m^2K)$	84,2	85,0	85,9	85,9
Kg	W/kgK	113,8	114,9	116,1	116,1
K_v	W/m^3K	75063,5	75737,5	76551,0	76551,0
η		0,908	0,892	0,870	0,870

	Dimension	Variants			
		1	2	1	2
		R1	R1	R2	R2
ΔLr_c	J/kg	517,00	517,10	517,5	517,5
ρ_2	kg/m^3	1,032	1,028	1,023	1,023

*Notes:

1. The designations match those provided in Table 3.6.

2. Calculations are performed for one partition of each radiator. In this case, values such as ΔP, ΔP_w, η and some others coincide with the data for the entire radiator.

Assessing the results of calculations with an increased charge air cooler, it can be stated that all the advantages listed above of the 2PK1M system over EC12A are preserved. The transition to an increased heat exchanger and the specified air temperature in the engine receiver does not alter these advantages either quali-?atively or quantitatively.

Thus, the proposed system proves to be significantly superior to the EC12A system.

Conclusions for the section.

Both considered cooling systems can maintain control temperatures for water and oil without violating dimensional constraints; the control air temperature can be achieved with a slight exceedance of the specified limits on the dimensions of the charge air cooler.

The proposed cooling system, 2PK1M, proves to be significantly superior to the EC12A system. The main advantages of the 2PK1M system are listed below.

- The total mass of the heat exchanger cores in the 2PK1M system (typically made of red copper) is almost 300 kg less than in the EC12A system (952 kg compared to 1249 kg, a difference of 297 kg). Consequently, the system's cost is also lower.

- 32 radiator partitions can be accommodated comfortably in the hood space of the BELAZ-7560 quarry dump truck, while fitting 46 partitions there is practically impossible.
- The proposed system is cooled by air with a flow rate of 60 kg/s, whereas the EC12A variant requires a flow rate of 80 kg/s.
- The EC12A cooling system is designed with two circuits (hot and cold), and accordingly, the charge air cooler has two bundles in one housing. The proposed 2PK1M cooling system has a single circuit and a simpler design of the charge air cooler (it has a single bundle).
- The EC12A system uses two water pumps, while the proposed 2PK1M system uses a single pump. In this case, the 2PK1M system is circulated with a correspondingly lower water flow (24.4 kg/s instead of 24.4 kg/s + 11 kg/s).
- Reducing the consumption of cooling air and cooling water lowers the energy consumption of the 2PK1M system during its operation (system energy efficiency).
- The system diagram is simpler.
- Temperature regulation of the heat carriers in the 2PK1M system is well-maintained. The variation in temperatures of all heat carriers, depending on the ambient temperature and engine operating conditions, is possible within wide ranges, covering the limits typically required for the optimal engine operation.

Section 4. Calculation of economic efficiency from the development and use of the designed system.

The transition of Ukraine to a market economy prompts a fresh look at the issue of quality, considering that the competitive market already dictates the level and dynamics of product quality development, determining the competitiveness of its manufacturers. According to the definition of the International Organization for Standardization, quality is a combination of properties and characteristics of a product that give it the ability to satisfy specified or presumed needs.

Quality stands as a key factor in the competitiveness of a product. The high quality and competitiveness of engine manufacturing are ensured by a marketing system - from design, prototype, and mass production, to sales and service of products, including installation and after-sales maintenance.

In this section, a technical and economic analysis has been conducted on the key indicators of the EC12A system (full-flow) compared to the 2PK1M system (low-flow).

4.1 Brief description of the EC12A and 2PK1M systems.

The cooling systems are applicable to the BELAZ-7560 mining dump truck.

The EC12A system (Fig. 4.1) is a two-pump system: one pumps the cooling liquid through circuit R1; the other pumps through R2. The system also includes a radiator device composed of locomotive radiator columns, a shell-and-tube oil cooler, 2 air charge coolers for hot and cold circuits, and a fan.

The 2PK1M system (Fig. 4.2) is designed on the principle of low consumption, meaning that not the entire volume of liquid pumped by the pump passes through each heat exchanger. The system also includes a radiator device composed of locomotive radiator columns, a shell-and-tube oil cooler, 2 air charge coolers for hot and cold circuits, and a fan.

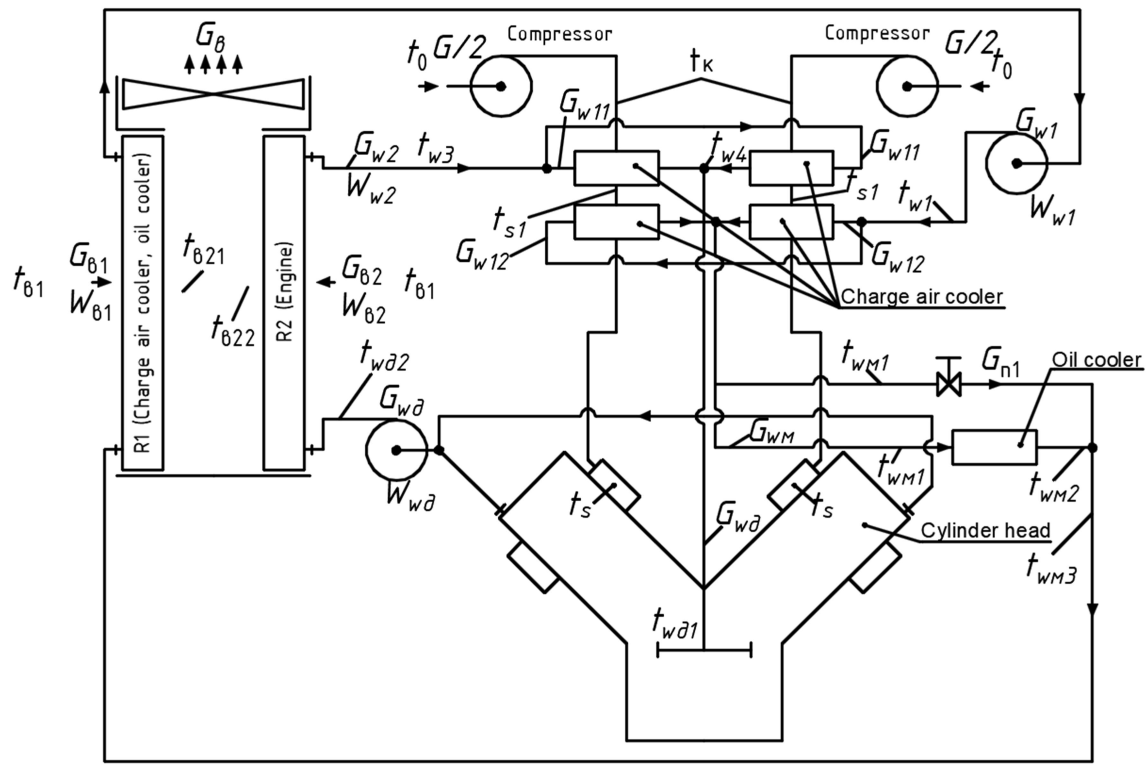

Figure 4.1 - Diagram of the EC12A Cooling System.

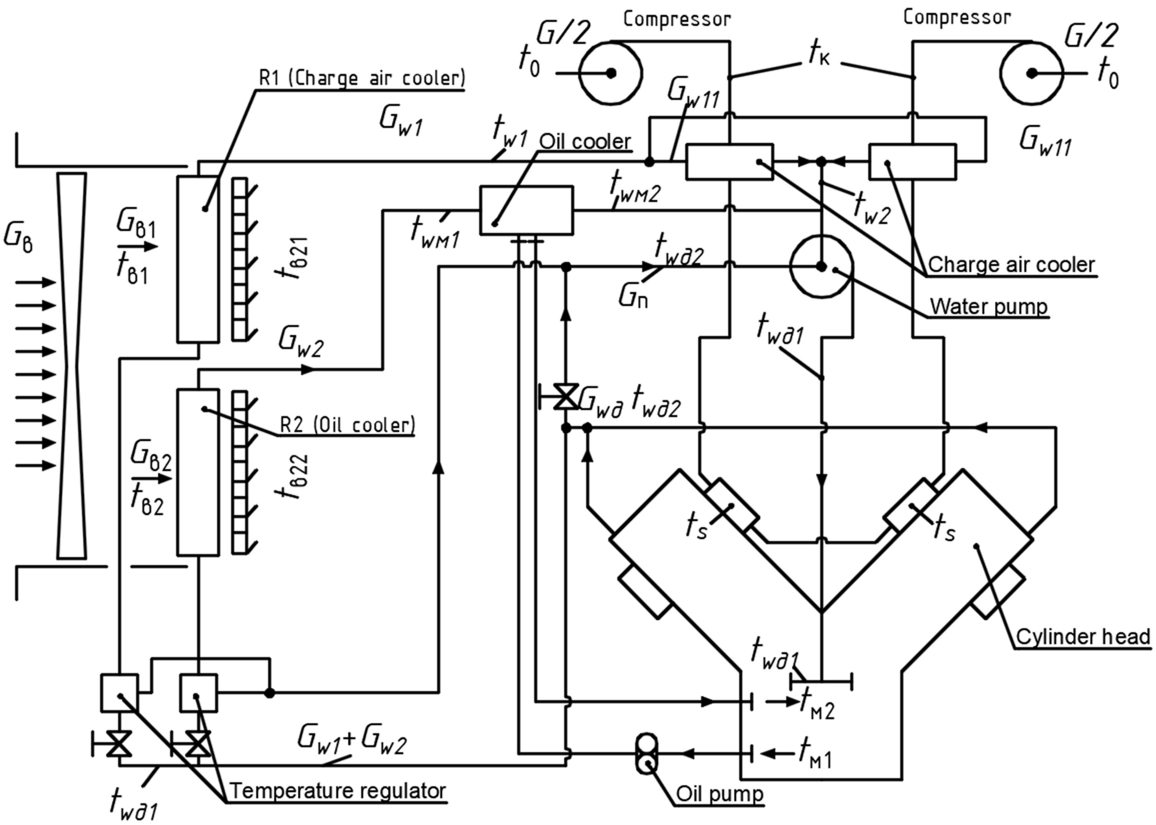

Figure 4.2 – Diagram of the 2PK1M Cooling System.

4.2 Justification of the economic efficiency of developing a low-consumption system.

In the 2PK1M system, the charge air cooler is a cooler with a single circuit of cooling liquid, unlike the EC12A system in which, structurally, the charge air cooler has 2 circuits. This allows the use of standard sizes of coolers from serial production in the system and eliminates the need for special (custom) manufacturing.

The 2PK1M system has a single water pump, as opposed to the 2 pumps in the proposed EC12A system. This reduces the layout costs of the system and simplifies it.

In both cooling systems, the radiator device consists of locomotive radiator columns. In the 2PK1M system, the number of columns 32 is fewer compared to EC12A 46, significantly reducing the system's cost and allowing for the placement of the radiator device in the vehicle's engine compartment.

The cores of the heat exchangers are primarily made from copper alloys. The average cost of 1 kg of copper is 240 UAH. The mass of the heat exchanger cores in the EC12A system is 1249 kg, compared to 952 kg in the 2PK1M system. The difference in mass is 297 kg. During the manufacturing stage of the heat exchangers, the cost savings amount to 71,280 UAH.

The designed 2PK1M system is more cost-effective, simpler in its design and maintenance, and more reliable, as it contains fewer elements than EC12A. However, 2PK1M is still capable of meeting the required parameters of the system's heat carriers.

					КРМ.142.6222м.01.05.ПЗ
Зм.	Арк.	№ докум.	Підпис	Дата	

Студент	Безушко С.О.			Section 5 Occupational Safety and Environmental Protection	Літ.	Аркуш	Аркушів
						69	10
Керівник	Мошенцев Ю.Л.				НУК		
Зав.кафед.	Гогоренко О.А.						

Section 5. Occupational Safety and Environmental Protection.

5.1 Occupational Safety

Occupational safety is a system of laws and regulations aimed at ensuring the safety of work, along with corresponding socio-economic, organizational, technical, and sanitary-hygienic measures.

The objectives of occupational safety are to minimize possible injuries and illnesses among workers while simultaneously ensuring comfort and maximizing labor productivity. Real working conditions are typically characterized by the presence of certain hazardous and harmful factors.

A hazardous production factor is defined as a factor whose impact on a worker under certain conditions leads to illness or a decrease in work capacity. The distinction between hazardous and harmful factors is not always clear-cut, as the same factor may result in an accident or a reduction in labor productivity.

5.1.1 Analysis of hazardous and harmful production factors affecting diesel service personnel

During the operation of internal combustion engines (ICE) and various systems and mechanisms servicing diesel engines, a range of production factors hazardous to human life and health arises. These factors are regulated by DSTU 12.0.003 - 83.

Fuel and oil vapors can penetrate the human body, causing irritation and potentially leading to the development of chronic respiratory diseases.

The operation of the engine also releases a significant amount of harmful substances as a result of the combustion of fuel and oil.

The temperature of open engine parts (exhaust manifold, gas turbine, muffler) can cause harm to humans, resulting in burns. To prevent this, it is necessary to cover all hot engine components with heat-insulating materials.

Fire safety. The causes of fires in the engine compartment include: malfunctioning electrical devices, spontaneous combustion of oily rags, malfunction of shut-off valves, wear and corrosion of fuel system components, the use of open flames, and failure to comply with fire safety standards when working with easily flammable substances.

Noise. Noise significantly impairs labor productivity and affects individuals. Prolonged exposure to high noise levels can result in fatigue of the auditory system, leading to partial or even complete hearing loss.

According to Sanitary Norm 2.2.4/2.1.8.562-96, the noise standard for workplaces of drivers and service personnel of tractors, self-propelled chassis, trailed and mounted agricultural machines, construction and road machinery, and other similar machines is 80 dB.

5.1.2 Calculation of noise and vibration level.

The noise level produced by the 12FC18,5/21,5 engine is determined by the formula:

$$L = \left[54 + 10 \cdot \lg\left(n_н + Ne^{0.55}\right) + 30\lg\left(\frac{n}{n_н}\right)\right], Дб$$

$n_н$ – nominal rotation speed, $n_н$ = 1900 rpm;

n – operating rotation speed, n = 1900 rpm;

N_e – nominal power of the engine, N_e = 2416 kW.

$$L = \left(54 + 10 \cdot lg(1900 + 2416^{\ 0.55}) + 30\, lg\left(\frac{1900}{1900}\right)\right) = 86.95, dB$$

The noise level exceeds permissible values, but if appropriate measures are taken to reduce it, the noise level will comply with standards.

5.1.3 Measures to reduce the noise level.

To mitigate the aerodynamic noise generated by the engine, various designs of mufflers are employed. The use of mufflers allows for a reduction in the overall noise level by 10 - 12 dB.

To decrease airborne noise emitted by the external surfaces of the engine, sound-insulating covers or enclosures are utilized, enabling a reduction in the overall noise level by 10 - 15 dB.

To diminish mechanical noise, it is necessary to reduce clearances between parts and assemblies, manufacture structures from materials with higher internal friction, and apply noise-absorbing coatings.

5.2. Environmental Protection.

5.2.1. General provisions.

Environmental protection is a system of legislative acts ensuring the normal functioning of the biosphere under the influence of natural or anthropogenic factors.

One of the necessary conditions for a healthy and highly productive work environment is ensuring the cleanliness of the air and normal meteorological conditions within the indoor working areas..

Preventing the impact of harmful production factors such as gas, vapor, dust, excessive temperature, and humidity, and creating a healthy air space is an important economic task that should be carried out comprehensively, simultaneously addressing the fundamental issues of production.

Harmful substances primarily enter the human body through the respiratory tract, as well as through the skin and with food. Most of these substances are classified as dangerous and harmful production factors because they affect the human body.

5.2.2. Environmental pollution during diesel engine operation.

During the operation, a diesel engine interacts with the environment, using air and water, and emitting exhaust gases into the atmosphere.

Let's consider the nature of the impact of components found in diesel engine exhaust gases on the human body. According to this criterion, hygienists divide them into 6 groups.

The first group includes substances that do not have a direct harmful effect on humans and the biosphere as a whole. These include nitrogen (N_2), oxygen (O_2), hydrogen (H_2), water vapor (H_2O), and carbon dioxide (CO_2).

The second group includes CO - carbon monoxide - a colorless gas without odor or taste, slightly lighter than air (density is 0.97 relative to air). It is practically insoluble in water. Flammable (forms explosive mixtures with air). When it enters a person's lungs, it displaces oxygen from the blood, as it has a solubility in blood 200 times greater than that of oxygen (reducing oxygen content in the blood leads to suffocation). The harmful effect of carbon monoxide on the human body is also explained by the fact that red blood cells - erythrocytes, capture CO and lose the ability to participate in the body's gas exchange. As a result, oxygen starvation occurs, leading to the disruption of the central nervous system, and in severe cases, death. At low concentrations in the air, it can cause dizziness and nausea. Since carbon monoxide has almost the same density as air (28 versus 28.7), it is poorly ventilated from enclosed spaces. The impact of carbon monoxide depends on its concentration in the atmosphere. At a concentration of 0.0016% by volume, the concentration is considered harmless. At 0.01%, there is a risk of chronic poisoning with prolonged exposure. A concentration of 0.05% can lead to mild poisoning within 1 hour. At 1.0%, there is a risk of loss of consciousness after several inhalations, and death may occur if the person is not removed from the air volume with such a concentration of carbon monoxide, and necessary assistance is not provided.

The third group includes nitrogen oxides, primarily nitric oxide (NO) and nitrogen dioxide (NO_2). Nitric oxide (NO) is a colorless gas, poorly soluble in water, and oxidizes to NO_2 in the air. Nitrogen dioxide (NO_2) is a red-brown gas with a distinct sharp odor, heavier than air. In equal amounts, nitrogen oxides are more toxic than CO. When they enter the human body and react with water, NO_x forms nitrous and nitric acids in the respiratory pathways, and their compounds destroy lung tissue, causing chronic diseases and irreversible changes in the cardiovascular NO_x also causes diseases of the mucous membranes of the upper respiratory tract, chronic bronchitis, and nervous disorders. In combination with hydrocarbons, they form toxic nitroolefins. Poisoning with nitrogen oxides has a hidden period, during which the poisoned person feels well, but later falls seriously ill.

Depending on the volumetric concentration in the air (in%), the impact of NO_2 on the human body is as follows:

- 0.00001: Absolute impact threshold

- Up to 0.0003: Threshold for taking action
- 0.0013: Threshold for irritation of mucous membranes
- Up to 0.002: Formation of methemoglobin
- 0.004 to 0.008: Pulmonary edema

Additionally, nitrogen oxides participate in photochemical reactions contributing to the formation of smog.

The fourth group, the most numerous, includes various hydrocarbons (compounds of the C_nH_m type), representing all homologous series: alkenes, alkadienes, cyclones, as well as aromatic compounds, including carcinogens. They have an unpleasant odor and can cause many chronic diseases, exhibiting a general toxic and irritating effect.

The fifth group includes aldehydes. They have a sharp odor, especially formaldehyde. At certain doses, they can cause irritation of the respiratory tract and mucous membranes of the nose and eyes. The impact on the human body is characterized by an irritating and general toxic effect on the central nervous system, affecting internal organs. In exhaust gases, formaldehyde and acrolein are mainly present.

The sixth group includes soot. Soot consists of the finest carbon particles ranging from fractions of a micron to ten microns; the smallest particles (not more than 10 micrometers) can linger in the air for days. Like any aerosol, soot pollutes the air, reduces visibility, and can irritate the respiratory tract. Carbon, as a chemical substance, does not pose an immediate danger to the human body. The main danger of soot lies in its role as a carrier of carcinogenic substances, specifically benzopyrene. Adsorbed on the surface of soot, benzopyrene has a stronger impact on living cells than in its pure form. Benzopyrene has been found not only in diesel soot but also in gasoline engine soot, containing 200 times more of this substance. However, the amount of soot in diesel engine exhaust is significantly greater than in gasoline engines.

In diesel engine exhaust, when using sulfur-containing fuels, inorganic gases are also present, which are sulfur compounds. They have a sharp odor, cause irritation of the upper respiratory tract, and disrupt protein metabolism in the body. Primarily, these are sulfur dioxide (SO_2) and hydrogen sulfide (H_2S). Sulfur dioxide is a colorless gas with a pungent odor, heavier than air (specific gravity to air is 2.264), soluble in water, and forms sulfuric acid. The impact of SO_2 on the human body depends on its volumetric content in the air, %, and can cause the following consequences:

- 0.0007 to 0.001: Throat irritation
- 0.0017: Eye irritation, cough
- 0.04: Poisoning within 3 minutes
- 0.01: Poisoning within 1 minute

Diesel engine exhaust gases, comprising 99.0 to 99.9% of fully combusted products (carbon and water vapor), residual oxygen, and nitrogen from the air. However, it is precisely the portion of exhaust gases that remain (not more than 1% of the total exhaust, practically equal to the air intake) that determines the environmental impact of engines, i.e., the degree of harmful effects on the environment: plant and animal life, humans, and architectural structures.

The main harmful components of diesel engine exhaust gases are nitrogen oxides, soot, and sulfur compounds. For gasoline engines, the toxic components include carbon monoxide, hydrocarbons, nitrogen oxides, and lead compounds (for leaded gasoline). Hydrocarbons emitted by gasoline engines enter the air with both exhaust gases and crankcase gases, as well as in the form of vapors from the carburetor and fuel tank. For diesel engines, the emission of hydrocarbons is usually associated only with exhaust gases. In gasoline engines, the overall amount of toxins in the exhaust gas is generally higher on average than in diesel engines. Moreover, there is a different proportion between the main toxins in the exhaust gas of gasoline engines and diesel engines.

In addition to harmful substances, the exhaust gas also contains nitrogen as ballast and carbon dioxide (CO_2). Regarding nitrogen, it is worth noting that, while it is not harmful to humans, it is a source of the formation of harmful oxides in the engine cylinder.

Carbon dioxide does not pose a noticeable threat to humans in open and well-ventilated spaces. Until recently, it was not considered a harmful component of engine exhaust gases. However, the production of carbon dioxide from fossil carbon fuels contributes to an increase in its concentration in the atmosphere. Carbon dioxide is among the so-called greenhouse gases in the atmosphere. Greenhouse gases have the ability to capture long-wave thermal radiation emitted by the Earth, which is not retained by other components of the atmosphere. Water vapor, methane, freons, and some other compounds are also considered greenhouse gases. Molecules of greenhouse gases absorb quanta of long-wave radiation, become excited, and then emit radiation themselves. This emitted radiation is directed in all directions, with half of the energy being sent into space, and the other half returning to Earth.

The action of greenhouse gases ensures the maintenance of certain equilibrium temperatures in the Earth's atmosphere and on its surface (for the atmosphere, the average annual temperature of the surface layer is +14°C). This equilibrium is the result of the thermal balance in the system Sun - Earth - Space. An increase in the quantity of carbon dioxide leads to an increase in the so-called greenhouse effect and may impact climate change on the planet. With the current rate of increase in the amount of this gas in the atmosphere (its mass fraction has increased from 0.00012 in 1912 to 0.00038 at the beginning of the new century), there is a possibility of raising the average annual temperature of the surface layers of the atmosphere by 2 to 4 °C in the next 100 to 200 years. This poses a threat of intensive melting of the planet's glaciers, a rise in the global sea level by 6 to 16 meters, and associated climate-related catastrophes.

One of the manifestations of the negative impact of transportation on the environment is smog. This term is widely used to denote visible air pollution of any kind (not only from transportation).

There are three main types of smog:

-Crystalline smog (Alaskan type) - a combination of gaseous pollutants, particulate matter, and ice crystals formed during the freezing of fog droplets and steam from heating systems.

-Simple smog (London type) - a combination of gaseous pollutants (mostly sulfur dioxide), particulate matter, and fog droplets.

-Photochemical smog (Los Angeles type, dry) - secondary air pollution that occurs as a result of the breakdown of pollutants under the influence of sunlight, especially ultraviolet.

The primary toxic component of smog is ozone (O_3). Additional constituents of smog include carbon monoxide, nitrogen oxides, peroxyacetyl nitrate, nitric acid, and some others. The main source of this type of smog is transportation.

All the mentioned substances (except soot) can lead to a fatal outcome when reaching a certain concentration in the air. Although the degree of harmfulness of these substances varies, and accordingly, there are different permissible concentrations of them in the air. Persistent exposure to humans, animals, and plants can lead to mutations at the genetic level and hereditary changes in organisms, altering their morphological (external and internal structure) and/or physiological-behavioral characteristics.

The impact of engine exhaust gases on plants is determined by the entry of exhaust gases both onto the surface of plants and into cells (with groundwater). Plants are particularly sensitive to sulfur oxides, nitrogen oxides, and compounds of nitrogen oxides with hydrocarbons. The impact of engine exhaust gases on buildings, monuments, and other architectural structures is also determined by the deposition of nitrogen oxide and sulfur oxide compounds on the surfaces of structural elements, as well as the deposition of oily particulate matter from soot.

5.2.3. The main ways to reduce the toxicity and smokiness of exhaust gases.

Improvement of operational processes and mixture formation. They enhance the turbulence intensity of the mixture in the combustion chamber, increasing the duration and power of the electric discharge, especially when operating on lean mixtures. This reduces CO emissions with rich mixtures but may increase NO_x emissions under nominal loads and lean mixtures.

Enhancements in fuel spray atomization under all operating conditions, including idle, forced idle, partial loads, and transient modes.

Improvements in the uniformity of fuel delivery to the engine cylinders. This involves the use of multi-chamber carburetors, fuel injection systems into the air receiver, intake manifolds, and directly into the engine cylinders.

Reducing the ignition advance angles decreases NO_x emissions but worsens engine efficiency and contributes to an increase in hydrocarbon and CO emissions.

Exhaust gas recirculation (EGR): A small amount of exhaust gas (10 to 12%, according to some sources up to 20%) is introduced into the intake pipeline after the carburetor during nominal operating conditions. This helps reduce NO_x emissions by approximately half by lowering the maximum combustion temperature (by 40 to 50% according to other data). The reduction occurs due to a decrease in the combustion reaction rate resulting from dilution of the combustible mixture with inert gases and a reduction in the mass of the fresh charge, consequently lowering the heat of combustion of the fuel. Simultaneously, there is a slight decrease in power and reduced engine efficiency. CO and CH emissions may slightly increase due to combustion process deterioration. It is considered that EGR is more advantageous during non-nominal modes, even though NO_x emissions are already low in these conditions. EGR is more effective for engines with a piston chamber than for engines with separated chambers.

Fuel and additives: Increasing the cetane number of the fuel improves the combustion process, reduces ignition delay, and decreases the cyclic variability and engine harshness. This results in a reduction in NO_x emissions, but it may increase smoke and hydrocarbon emissions. Increasing the light fractions in the fuel enhances its vaporization, improving the uniformity of fuel distribution throughout the combustion chamber volume. This reduces all types of emissions. Additives to diesel fuel, such as organometallic additives based on barium, manganese, and tetraethyl lead, allow for a several-fold reduction in exhaust smoke and the content of aldehydes and benzopyrene at high loads. Smoke reduction for an undivided combustion chamber diesel is in the range of 40 to 90%. Additives do not affect nitrogen oxide emissions. A significant portion of barium combines with sulfur in the fuel, releasing into the atmosphere as a relatively harmless barium sulfide. Two hypotheses for the action of additives have been proposed: the first suggests inhibition of soot particle formation during combustion, while the second proposes that smoke reduction is achieved through the catalytic action of additives during the oxidation of soot particles during diffusion combustion, expansion, and exhaust. The use of low-lead-content gasoline allows influencing the emission of lead compounds and significantly extending the service life of catalytic converters.

Engine conversion to gaseous fuel allows for a roughly two-fold reduction in NO_x emissions and a slight decrease in CO emissions. This is due to the fact that when running on gas, it is possible to efficiently use leaner mixtures that combust at lower temperatures. Additionally, the uneven mixture composition across the engine cylinders is reduced.

Exhaust Gas Neutralization: The level of toxic substance emissions in exhaust gas can be reduced through the neutralization of gases in specialized devices called neutralizers. Neutralizers are installed at the exhaust gas outlet from the engine cylinders and are designed to convert toxic substances into non-toxic ones or to capture (absorb) toxic substances. Accordingly, there are thermal, catalytic, and mechanical neutralizers. Thermal and catalytic neutralizers involve chemical reactions that result in a reduction in the concentration of gas components of toxic substances.

Conclusion for the project

The master's thesis has been completed in accordance with the department's assignment on the topic: "Selection of a rational cooling system DM-185 type engine for a quarry dump truck"

The system proposed by BerMP includes the following elements: a radiator assembly, an oil cooler, an intercooler, two water pumps, and a fan.

The radiator is assembled from standard locomotive partitions. As a result of a detailed calculation of the EC12A cooling system, the value of radiator partitions was determined to be 46, which cannot fit into the underhood space of the vehicle.

The Charge air cooler consists of 2 parts, meaning it has 2 circuits running through it. Such a cooler is not produced in series, and consequently, it is manufactured individually. A two-circuit system entails the use of 2 water pumps.

It is evident that the system does not meet modern engine-building standards. Therefore, the decision was made to design a new system.

Based on the EC12A, a low-flow cooling system, 2PK1M, was designed. The system has a single water pump, which significantly reduces the cost of layout and maintenance. It has 32 partitions, which, in turn, easily fit into the vehicle's underhood space. The intercooler has a single circuit, allowing the use of off-the-shelf heat exchangers. At the same time, the system is capable of meeting all specified parameters of the coolants. The main parameters of the systems and their elements are presented in Table 6.1.

Table 6.1. The main parameters of the systems and their elements.

Parameter	Dimension	EC12-A		2PK1M		Note
		1	2	1	2	
$G_в$	kg/s	80	80	60	60	Air flow rate by the fan
G_w	kg/s	35,5	35,5	28,6	29,4	Total water flow rate in the system
Zc .	pcs	46	46	32	32	Total number of radiator panels
T_s	°C	54	45	54	44,9	Air temperature in the receiver
$T_{wд1}$	°C	101,3	100,1	104	104	Water before the diesel engine

$T_{wд2}$	°C	105,3	104	108	108	Water after the diesel engine
M_{Σ}	kg	1184	1249	885	952	Total mass of all heat exchangers
η_{co}		0,907	0,949	0,907	0,949	Cooling system efficiency
$T_{м1}$	°C	90,6	90,2	89,9	89,9	Oil temperature before the engine
$T_{м2}$	°C	105,3	104	96	96	Oil temperature after the engine
$G_{м}$	kg/s	14	14	14	14	Oil flow rate

In Section 1, the application of the 12FC18,5/21,5 engine with the 2PK1M cooling system on a quarry dump truck is considered, along with their placement in the vehicle's underhood space.

In Section 2, the working cycle of the 12FC18,5/21,5 engine is simulated. The engine parameters obtained from the simulation are comparable to those of engines of a similar size and power. The thermal flows necessary for further system calculations are also obtained.

Section 3 provides a detailed examination and calculation of each cooling system scheme. The constraints specified in the technical assignment are taken into account. It is worth noting that the calculations are carried out for two variants. The first variant maintains the geometric dimensions of the intercooler specified by BerMP. In the second variant, the calculations are performed with slightly increased dimensions of the intercooler.

List of References:

1. В.Г. Дяченко. ДВИГУНИ ВНУТРІШНЬОГО ЗГОРЯННЯ, ТЕОРІЯ. Підручник для студентів вищих навчальних закладів. Харків НТУ «ХПІ» 2008 – 488с.

2. Blitz-PRO by D. S. Minchev. User’s manual.

3. Donatello A. Handbook for heat exchangers and tube banks design. 2010 – 185 s.

4. Анастасенко С.М. Теплообмінні апарати. 2023 – 228 с.

5. Кириленко О. П. ОСНОВИ НАУКОВИХ ДОСЛІДЖЕНЬ У СХЕМАХ І ТАБЛИЦЯХ. Навчальний посібник. Тернопіль 2013 – 288с.

6. . Standards of TEMA 9th edition. 2007 – 298 s.

7. СИСТЕМА КОНСТРУКТОРСЬКОЇ ДОКУМЕНТАЦІЇ. Терміни та визначення основних понять, ДСТУ 3321:2003, Київ 2005. – 55 с.

8. І.П. Пістун. Охорона праці в галузі машинобудування, навчальний посібник. 2012 - 558 с.

9. О.І. Іваненко, Ю.В. Носачова. Техноекологія: підручник. Київ: Видавничий дім «Кондор», 2017. — 294 с.

10. Михайлюк В.О., Ізотов В.І., Штейн П.В. Методичні вказівки до виконання розділу з питань безпеки життєдіяльності та цивільної оборони у дипломних роботах (проектах) студентів. – Миколаїв: НУК, 2009. – 56 с.